Research Report R81-5

RAPID QUENCHING EFFECTS IN PVC FILMS

by
H.-D. LEE
J.F. MANDELL
F.J. McGARRY

October 1981

MIT

DEPARTMENT OF MATERIALS SCIENCE AND ENGINEERING

SCHOOL OF ENGINEERING
MASSACHUSETTS INSTITUTE OF TECHNOLOGY
Cambridge, Massachusetts 02139

D 82N33524

DISPLAY 82N33524/2

82N33524*# ISSUE 24 PAGE 3413 CATEGORY 27 RPT#: NASA-CR-169350 NAS
1.26:169350 MIT-R81-5 81/10/00 73 PAGES UNCLASSIFIED DOCUMENT

UTTL: Rapid quenching effects in PVC films

AUTH: A/LEE, H. D.; B/MANDELL, J. F.; C/MCGARRY, F. J.

CORP: Massachusetts Inst. of Tech., Cambridge. CSS: (Dept. of Materials Science and Engineering.)

AVAIL.NTIS SAP: HC A04/MF A01

Sponsored by NASA

MAJS: /*MECHANICAL PROPERTIES/*POLYMERIC FILMS/*POLYVINYL CHLORIDE/*QUENCHING (COOLING)/*THIN FILMS

MINS: / COOLING/ GLASS/ MOLECULAR STRUCTURE/ POLYMERS/ VINYL POLYMERS

ABA: Author

ABS: Using a specially constructed microbalance for hydrostatic weighing, density changes in PVC thin films (with no additives, 30-100 micrometers thick), due to rapid quenching (approximately 300 C/sec) through the glass transition temperature, have been observed. The more severe the quench, the greater is the free volume content. Isobaric volume recovery of PVC has also been studied by volume dilatometry. Both show aging or relaxing molecular rearrangements takes place as a linear function of logarithmic aging time at room temperature. Distribution of retardation times and Primak's distributed activation energy spectra have been applied to the volume recovery data. The concomitant changes in mechanical properties of PVC after quenching have been monitored by tensile creep and stress-strain

MORE ENTER:

RESEARCH REPORT R81-5

RAPID QUENCHING EFFECTS IN PVC FILMS

by

H.-D. Lee
J.F. Mandell
F.J. McGarry

October 1981

Sponsored by
National Aeronautics and Space Administration Headquarters
Materials Processing in Space Division

School of Engineering
Massachusetts Institute of Technology
Cambridge, Massachusetts 02139

ABSTRACT

RAPID QUENCHING EFFECTS IN PVC FILMS

Using a specially constructed microbalance for hydrostatic weighing, density changes in PVC thin films (with no additives, 30~100μ thick), due to rapid quenching (~500^{o}C/sec) through the glass transition temperature, have been observed. The more severe the quench, the greater is the free volume content. Isobaric volume recovery of PVC has also been studied by volume dilatometry. Both show aging of relaxing molecular rearrangements takes place as a linear function of logarithmic aging time at room temperature. Distribution of retardation times and Primak's distributed activation energy spectra have been applied to the volume recovery data.

The concomitant changes in mechanical properties of PVC after quenching have been monitored by tensile creep and stress-strain to failure. All reflect the presence of excess free volume content, due to rapid quenching.

INTRODUCTION

Recently, metallic glasses prepared by quenching molten alloys at the rate of approximately 10^6 ^oC/sec have been intensively studied (1-6). Such materials are characterized by amorphous state, ductility, lower modulus of elasticity, high flow stress, superior fatigue resistance, higher electrical resistivity, superior corrosion resistance, etc.

Compared to metals, polymers exhibit not only relatively poor thermal conductivity but also a narrower temperature range for quenching. Accordingly, similarly high quenching rates are not possible for polymers. Using thin film specimens of glassy polymers and selecting adequate quench media, however,relatively fast cooling rates in the range of 500-700 ^oC/sec can be achieved. According to the concept of fictive temperature (7, 8) it is believed that the fictive temperature, where glass formation begins, will be greater at increasing cooling rates (7, 8, 9). In this connection, excess free volume that is required for segmental motion will be frozen in. Subsequently, when such a quenched glassy polymer is aged at a temperature below T_g , densification and change in the population of the various conformational isomers of the polymer chains will ensue in order to reach an equilibrium state. The reduction in the excess free volume, thus, results

in a significant observed embrittlement of amorphous polymers (10, 11, 12).

In the pioneering studies regarding the influence of aging on the mechanical properties of amorphous polymers (13), it was concluded that the changes in dynamic shear properties of poly(vinyl acetate) during both isothermal contraction and expansion can be correlated with the characteristic volume recovery behavior. More recently, Struik (14, 15) suggested that aging is a basic phenomenon in solid materials in a temperature range between the β-relaxation and the glass transition. In contrast to Petrie (16, 17), Struik considered the secondary relaxations to be unaffected by aging, although he attributed certain effects to changes in the low temperature tail of the glass-transition peak, i.e., to primary relaxation phenomena. Combined with other studies (17-22), it is quite clear that the effect of annealing or aging is to reduce the free volume content due to the normal liquid-like packing of chains.

Theoretical and experimental results reported by Williams, Landel and Ferry (23), Turnbull and Cohen (24) and Kovacs (25) suggest that molecular transport mobility depends on free volume. It turns out that the correlationship among free volume,

volume recovery, molecular mobility, and mechanical behaviors can be easily understood from the following:

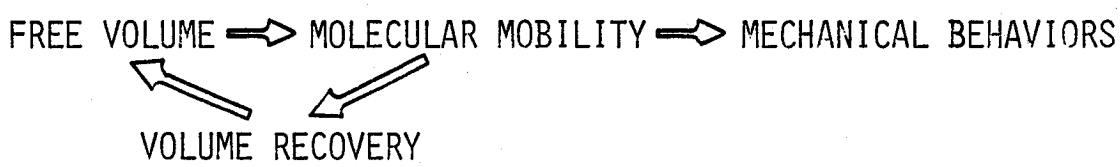

Although various degrees of success have been achieved by utilizing thermodynamics, phenomenological modeling, or a combination of both in an attempt to describe the nonequilibrium behavior of glassy polymers, a correlation between molecular behavior and observed macroscopic properties must be made in order to gain a complete understanding. Recently, Robertson (26, 27) has suggested that the recovery process can be described by the approach of the conformational degrees of freedom of the polymer backbone toward equilibrium. It is assumed that the rate of conformational change is dependent upon the fractional free volume within the environment of the transforming segment just as the macroscopic relaxation depends on the average free volume. More specifically, conformational changes occur only in regions of sufficient free volume which are varied by thermal fluctuations. Using a five-bond model consisting of cis and trans backbone rotational states, he computed the τ_{eff} behavior of polystyrene as a

function of the departure from volumetric equilibrium by means of a typical set of material paramenters. Although these results cannot be directly compared to Kovacs' results (28-33) for poly(vinyl acetate), the τ_{eff} behavior yielded from this molecular model is quite similar to the poly(vinyl acetate) data, provided the difference in the T_g's of the two polymers are taken into account. In spite of the shortcoming regarding prediction of the dependence of equilibrium states on previous thermal history evidenced by Kovacs's data the contribution of this molecular model in qualitatively describing the complex τ_{eff} behavior is important to the understanding of the glassy state and nonequilibrium behavior.

However, the above-mentioned studies still lack technological implications, especially for rapid quenching effects, on its concomitant mechanical properties. More specifically, the role of excess volume in the ductility of glassy polymers must be defined in order to gain further insight into the modes of molecular motion that contribute to the observed ductile behavior. Based on this understanding, it is hoped to predict the changes in material properties and further to utilize the benefits of rapid quenching effects for glassy polymers as engineering materials. Thus, intensive study regarding rapid quenching effects on the mechanical properties of amorphous polymers has been undertaken and proposed for further work.

OBJECTIVE

The objective of this research is to study the effects of rapid quenching on the concomitant mechanical properties of some glassy polymers. More specifically, it is trying to gain further insight into this subject in terms of free volume concept, molecular configuration, and mechanical properties.

PRELIMINARY WORK

EXPERIMENTAL

MATERIALS

In order to achieve the highest cooling rates, thin film specimens of polyvinyl chloride (Geon 121) which contains no additives, are prepared either by solvent-casting in T.H.F. or by melt-molding. Typically, film thickness is in the range of 30μ to 130μ.

Attention must be given to the amount of residual T.H.F. in the solvent-cast films even though specimens were subjected to vacuum at 60°C for 72 hours. The melt-molded films were obtained by pressing the dry powder under 700-800 psi at 190-220°C for 30-60 seconds. All specimens were then exposed to a series of annealing cycles to determine either the amount of residual T.H.F. in solvent-cast films or the possible thermal degradation of PVC.

ANNEALING AND QUENCHING

During annealing and quenching, the specimens were wrapped in aluminum foil (0.02 mm thick) and copper sheet (0.13 mm thick), as shown in Figure 1,in order to prevent surface contamination and to maintain good shape for mechanical tests. The temperature for annealing was in range of 90°C to 160°C at atmospheric pressure. The time for annealing was 3-6 minutes. To detect the temperature change against time during quenching or annealing, a thermocouple was inserted into the sandwich shown in Figure 1. The cooling rates were then obtained and shown in Figure 2.

APPROACHES FOR FREE VOLUME STUDIES:

HYDROSTATIC WEIGHING

Among the methods available for density measurements, hydrostatic weighing is the best approach for fast measurement and accuracy (34, 35). This method consists of weighing an object of known mass while it is suspended from a balance in distilled water which has been boiled to degas the trapped air (36). The indicated loss of mass being equal to the mass of displaced liquid, accordingly, it is possible to calculate the volume of the object (37, 38, 39).

The use of thin film specimens has two serious disadvantages: the weight is only 100 mg and the large surface area causes serious static electricity problems. Accordingly, to monitor density changes to ± 0.0001 gms/cm^3, not only a very high sensitivity balance but a big chamber to minimize static between the specimen and chamber wall are required.

Following the ideas of Madorsky (40), a microbalance was constructed to perform the hydrostatic weighing. As shown in

Figure 3, this employs a quartz spring or a fine tungsten wire in the form of helical spring. In order to reduce the variability in the downward surface tension force (36), the suspension wire which has a diameter of 7μ was treated as shown in Figure 4. The result of electrical heating under $1\sim10\times10^{-3}$ torr vacuum yields a uniformly granular coating of chromium oxide on the surface of the nichrome wire. Further, a precision thermoregulator shown in Figure 5 was made to control the temperature of the distilled water within $\pm0.005^{\circ}C$. Consequently, using a cathetometer which reads to 10μ, the balance can detect weight differences of 5×10^{-6} gms., giving the desired density sensitivity of 0.0001 gm/cm^3 or better.

APPROACHES FOR FREE VOLUME STUDIES:

DILATOMETRY

The volume recovery behavior under various temperatures is studied by a glass dilatometer described in detail by Bekkedahl (41). This consists of a reservoir, containing the specimen of known mass, joined to an accurately calibrated capillary of known cross-sectional area. The technique of filling mercury has been improved by employing a specially designed mercury reservoir, shown in Figure 6, instead of a three-way stopcock. This results in $1x10^{-4}$ torr vacuum or better to give highly reproducible data. Standard corrections are applied to allow for the expansion of the mercury, the glass, and the trapped gas. The specimen is then subjected to different thermal treatments by immersing the dilatometer in the glycerine bath, which is thermostatically controlled to within $\pm 0.05^{\circ}C$ in the range of $80^{\circ}C$ to $130^{\circ}C$, and the water bath, which is controlled by the thermoregulator within $\pm 0.005^{\circ}C$ in the range of 20° to $82^{\circ}C$. Finally, using a cathetometer read to 50μ, this set-up as shown in Figure 7 can detect volume changes to $1x10^{-5}$ cm^3.

APPROACHES FOR THE STUDIES IN MECHANICAL PROPERTIES:

STRESS-STRAIN TO FAILURE

To determine the yield stress, elongation at break, and ultimate strength of the specimens, tensile tests were made on the Instron using a crosshead speed of 0.5 in/min. The specimen dimensions are 0.394 in. width and 1 in. in length with thickness approximately 50 μ.

APPROACHES FOR THE STUDIES IN MECHANICAL PROPERTIES:

TENSILE CREEP

Because of the thin film nature of the specimens used, it was necessary to construct a special apparatus to perform creep measurements. This required careful temperature control and optical determination of strain because a mechanical extensometer would disturb the response of the specimen. The apparatus is shown schematically in Figure 8. Further, an aluminum foil sample was employed for proof testing.

RESULTS

WEIGHT LOSS AND DENSITY MEASUREMENTS DURING VARIOUS ANNEALING CYCLES

Although there is no indication from the IR analysis showing that residual solvent is retained in solvent-cast films, it is suspected that a significant amount of T.H.F. still exists in the specimens. Evidence is obtained from the study concerning the weight loss of solvent-cast films subjected to various annealing cycles at 140°C. Detailed results shown in Figure 9-a and 9-b, which represent the percent of weight loss and the corresponding density at various annealing cycles, respectively, confirm this.

In the case of melt-molded specimens, Figure 10-a shows that there is no weight loss after a few annealing cycles. The corresponding density measurements shown in Figure 10-b again reflects this observation. It is apparent that weight and density of melt-molded films are not much affected by short time annealing. In essence, the thermal degradation of PVC during short times and below 150°C annealing can be ignored.

To conclude this part of work, it is clear that attention must be given to the amount of residual T.H.F. retained in the

solvent-cast films. Only specimens which do not show any weight loss or density changes during short time annealing, for instance 3 min at 150°C, can be subjected to further tests regarding volume recovery and mechanical testing.

DENSITY MEASUREMENT AND DENSIFICATION STUDIES BY HYDROSTATIC WEIGHING

With the microbalance constructed and operating satisfactorily, it became possible to direct efforts to investigate the excess free volume content due to rapid quenching effects. Following the thermal history shown in Figure 2, a melt-molded film specimen (Geon 128) with thickness about 0.12 mm was subjected to either air cooling or rapid quenching to $0^{\circ}C$ ice water from $100^{\circ}C$. Specific volume measurement and subsequent densification against logarithmic time were obtained by means of hydrostatic weighing. The results shown in Figure 11 reveal two important observations: first, only a small amount of excess free volume (less than 0.02 %) is trapped in the glassy matrix due to different quenching rates between ice water quenching and air cooling; second, densification takes place as a linear function of logarithmic aging time at room temperature.

Further, the effect of the quench range was studied by quenching a melt-molded film specimen (0.22 mm thick, Geon 121) from various initial temperatures to ice water. As shown in Figure 12, more of the excess volume characteristic is retained when quenched from a higher temperature. Again,

densification due to physical aging takes place almost as a linear function of logarithmic aging time at room temperature.

DILATOMETRIC DATA

To gain further understanding regarding the volume recovery and the glass transition of PVC, volume dilatometers have been intensively used for higher temperature studies. Specific volumes at equilibrium states obtained from this method are plotted against temperature and shown in Figure 13. This demonstrates that the equilibrium state is attained almost instantaneously beyond 90°C. As the temperature is lowered to the range of 78~90°C, which is near the glass transition temperature of PVC, however,the equilbibrium structure is not obtained within 20 minutes. In the range of equilibrium states, a slope of 4.036×10^{-4} $cm^3/°C$ results for the thermal expansion coefficient above the glass transition of PVC.

To construct isochronal volume versus temperature curves it is necessary to carry out volume recovery at various final or aging temperatures. This is dilatometrically performed by quenching PVC specimen from 99°C, where PVC is characterized by an equilibrium structure, to various temperatures: 20°C, 30°C, 40°C, 44.9°C, 50°C, 55°C, 60°C, 65°C, 70°C, 74°C, 76°C, 78°C, 80°C, 80.5°C, 81°C, and 82°C. The volume recovery behaviors in the temperature range of 20°C to 65°C, which is far below

the glass transition temperature of PVC, are shown in Figure 14. Similar results of volume recovery behavior near the glass transition temperature of PVC are shown in Figure 15. In both graphs, the relative excess volume $(V - V_\infty)/V_\infty$ represents a dimensionless measure of the departure from equilibrium. The straight lines of Figure 14 plotted in semilogarithmic form indicate a tendency for the rate of contraction to become slower as contraction proceeds with time. Furthermore, the relative excess volume retained at various temperatures is proportional to the temperature difference. Accordingly, the volume recovery behaviors at temperatures from 20°C to 65°C, which are far below T_g of PVC, are linear and show no transition stage through a 400-hour observation interval.

However, the contraction isotherms shown in Figure 15 display both a transition stage and non-linearity in the vicinity of the glass transition temperature. In addition, the very shallow slope of the isotherm volume recovery behaviors indicates a slow approach to equilibrium, so that molecular rearrangements do not reach an equilibrium state within 400 hours, even at a temperature as high as 82°C.

Consequently, two ischronal branches below the equilibrium state, measured at 1 minute and 200 hours after quenching

from equilibrium at 99°C to various temperatures T, are constructed and shown in Figure 16. Both branches asymptotically approach two parallel straight lines with a slope of $\bar{\alpha}_g=(d\ v/d\ T)_t=7.35\times10^{-5}$ $cm^3/°C$. These lines intersect the equilibrium volume line at 83.3°C and 80.9°C, which can be associated with the glass transition temperatures T_g^t at 1 min and 200 h, respectively.

Another set of isothermal experiments to investigate the amount of possibly trapped excess free volume due to quenching effects was conducted by quenching from different initial temperatures to the same final temperature, 20°C. The results shown in Figure 17 reveal three important observations: first, 40 seconds are required to establish thermal equilibrium; second, a transition stage is observed in the range of 78°C to 99°C; and third, the more severe the quench, the greater is the free volume content. Accordingly, almost no excess free volume will be trapped from quenching below T_g to the lower temperature.

MECHANICAL PROPERTIES OBTAINED FROM STRESS-STRAIN TO FAILURE STUDIES

Stress-strain to failure were studied by quenching the solvent-cast film specimens from 118°C to liquid nitrogen in which the specimens were held for three minutes. Upon warming to room temperature, 20~25°C, tensile tests were then carried out at various aging intervals up to 220 hours. The results of engineering stresses and elongation at break are plotted verus aging time as illustrated in Figure 18. At early aging times, yielding is accompanied by necking, orientation, extensive cold drawing and very significant work hardening. Being calculated on the original cross-sectional area, the ultimate stresses and the yield stresses are in even greater error than the case of homogeneous deformation as localized thinning or necking occurs. However, it is apparent that the fracture or ultimate load exceeds the yield load even with a greatly reduced cross section. As aging continues, the neck disappears and the yield stress increases whereas the ultimate stress decreases. Both the extensive cold drawing and the work hardening diminish, until, eventually a very different kind of stress-strain behavior is exhibited. In essence, a transition from a general ductile behavior to brittle fracture is observed from aging the quenched PVC thin film specimens.

MECHANICAL PROPERTIES OBTAINED FROM TENSILE CREEP

To perform the proof testing of the creep apparatus which is schematically shown in Figure 8, an aluminum foil specimen was subjected to 1200 psi at room temperature. As expected, no creep was observed from Figure 19 within 44 hours. In contrast, two PVC specimens, which were annealed at 98^{o}C for one hour and then cooled slowly, exhibited measurable creep under 1700 psi over a similar time interval. Detailed results are also shown in Figure 19. It is clear that both PVC specimens behaved identically under the same conditions. In this connection, it is important to point out that the stress 1700 psi is in the linear region for unplasticized PVC (42). As suggested by Findlay et al. from extensive experimental studies on several thermoplastics (43, 44, 45), the theoretical curve can be plotted in the form of $\varepsilon(t)=\varepsilon_o + \varepsilon^* t^n$, where, t is time, ε_o is the time-independent strain, ε^* is the coefficient of time-dependent term, and n is a constant independent of stress. Unfortunately, this equation assumes the system is in equilibrium and it ignores any aging effect which could produce changes. Accordingly, it becomes increasingly inaccurate with increasing aging time under the same stress.

To gain further insight into how the rapid quenching will

affect the molecular mobility, the creep behaviors were studied by subjecting the specimens to different thermal histories. In Figure 20, Test #1 of both Sample 1 and Sample 2, which were quenched from 96°C to 0°C ice water, show identical creep behavior. As compared to the air-cooled sample, Test #2 of Sample 1, a great difference in creep is observed. The higher free volume content of the quenched samples confers much greater molecular mobility resulting in the greater initial extension and a greater rate of creep, whereas a higher density characterizes the slow-cooled sample so that reflects less instantaneous strain and less subsequent creep. In addition, the sequence of tests on Sample 1, ice-water quenching/air cooling/ice-water quenching, clearly discloses the thermoreversibility of the phenomenon: a slow creep behavior can be erased by subsequent ice-water quenching to cause a reversion to the original higher creep. Finally, Figure 20 also implies that the effects of different aging times, 9, 10, and 11 minutes, on the creep behavior are too small to be observed at room temperature.

The concept of diminishing free volume in the glassy polymer has been studied by aging the quenched sample (from 96°C to ice water) at room temperature for various aging intervals, in the sequence of 18, 36, 9, 153, 214, and 10 minutes prior to loading. The results shown in

Figure 21 not only confirm the thermoreversibility, despite the sequence of testing but also illustrate a great difference in the creep behavior caused by various aging intervals. For instance, after aging for 205 minutes which is the time difference between 214 minutes and 9 minutes prior to loading, nearly a 50 % difference in the compliance or the modulus of the PVC can be seen at 5000-second creep. During this 205 minute aging interval, 0.077 % volume contraction calculated from the linear measurements of specimen dimensions is in good agreement with data obtained from hydrostatic weighing. In a sense this can be interpreted as excess free volume diminishing in the glassy matrix as an equilibrium structure after quenching is approached. Its effect on molecular mobility is large.

If the initial temperature from which the material is quenched is varied while the aging interval is held constant, the creep should behave like that of being subjected to various aging intervals while having the same quenching condition. Experimently, this is clearly demonstrated in Figure 22. The quench from 153^{o}C to 0^{o}C produces the least dense structure and the highest creep values, whereas the quench from 96^{o}C to 0^{o}C gives the most dense structure leading to the lowest creep. In essence, quenching from

various temperatures above T_g to ice water clearly produces different levels of instantaneous creep and its subsequent creep at the same aging time prior to loading. It turns out that the creep behaviors presented in Figure 21 and Figure 22 are similar, by superposition. Consequently, the level of excess free volume trapped in the glassy matrix becomes the intrinsic factor to determine its concomitant changes in physical properties. More specifically, the aging effect is essentially a phenomenon caused by the change of molecular rearrangements.

DISCUSSION

When a PVC thin film specimen is rapidly quenched from above T_g to ice water or a lower temperature, excess free volume will be trapped in the glassy matrix as confirmed by the hydrostatic weighing and the dilatometry. Further, this trapped excess free volume tends to diminish as a result of relaxing molecular rearrangements. As treated by Tool et al. (7, 8) and Kovcas et al. (32, 46), the fictive temperature T* can be defined

$$T^* = T + (v - v_\infty)/\Delta\alpha v_\infty$$

where, T is an experimental temperature lower than T_g,

v is the nonequilibrium volume at T,

v_∞ is the equilibrium volume at T, and,

$\Delta\alpha$ is the excess thermal expansion coefficient between the liquid state and the glass state.

Due to the aging effect, the isobaric volume v is approaching the equilibrium volume v_∞ under isothermal contraction and the glass transition of long-time aged glassy polymer should move to a lower temperature as compared to that of short-time age after quenching. This is clearly illustrated in Figure 16: the T_g^t of PVC is shifted from 83.3° to 80.9°C as the aging interval is increased from 1 minute to 200 hours. In fact, T_g^t appears as the fictive temperature of the nonequilibrium

glass for which configurational changes toward equilibrium proceed for a duration shorter than the experimental time scale t. Similar results were obtained and plotted in Figure 23. The most significant feature of this Figure is that the shift of glass transition temperatures takes place as a linear function of logarithmic aging time. The explanation for this can be clearly seen in Figure 14 and Figure 15 from which a linear behavior is observed (during the experimental time scale) to dominate the isothermal volume contraction at the glass state except in the vicinity of the glass transition temperature.

Utilizing a single parameter model to characterize the rate of approaching the equilibrium state, Kovacs (29) proposed the equation

$$\tau_{eff}^{-1} = - \delta^{-1}(d\ \delta/d\ t)$$

in order to express the instantaneous effective retardation time τ_{eff} for isotherms. Further, a multiparameter model based on a distribution of retardation times (29, 30, 47) has advanced the study regarding nonequilibrium phenomenon of glassy polymers in the aspects of asymmetry behavior between the cooling isobars and the heating isobars, the nonlinearity of the glass transition, and the memory effects.

In this model each isothermal recovery follows the equation:

$$\tau_i^{-1} = -\delta_i (d\,\delta_i / d\,t)$$

where, $1 \leq i \leq N$; $\sum_{i=1}^{N} (d\,\delta_i / d\,t) = d\,\delta / d\,t$; and $\sum_{i=1}^{N} \delta_i = \delta$

As treated by this model, the discrepancy between the experimental expansion isotherms and theoretical plots (29, 30, 32) tends to vanish as $|\delta|$ approaches zero. In contrast, no noticeable discrepancy observed from the contraction isotherms implies that the intrinsic contraction behavior is associated with a single parameter model or the free volume theory. Thus, the intrinsic contraction isotherms, shown in Figure 24 and Figure 25 both exhibit a rapidly increasing retardation time which is required for a diminishing δ. Another important feature is that a nearly linear behavior characterizes the observed τ_{eff} except in the vicinity of T_g. This phenomenon does not contradict the nonlinear nature of volume recovery because a wide range of T-jumps and lower final or aging temperatures associated with the experiments result in a broad stabilization period or large linear region.

The nonequilibrium behavior in glassy polymers can be studied by the activation energy distribution

analysis which has been developed by Vand (48), Primak (49, 50), and expanded by Kimmel and Uhlmann (51, 52). The general differential equation (52) describing the aging of a property p with an equilibrium value p_∞ can be written

$$- d\,p(t)/d\,t = A\, e^{(E/KT)(p(t)-p_\infty)^n}$$

where, p(t): the value of the property at time t,

p_∞ : the value of the property at equilibrium,

A : frequency factor (10^7~10^9 sec^{-1}),

E : activation energy,

K : Boltzmann's constant,

T : temperature, and

n : the order of the process.

The approximate expression for this differential equation has been expressed in terms of the activation energy spectrum

$$p_{O\infty O}(E) = - \frac{1}{RT} \frac{d\,p(t)}{d\,\ln\,t}$$

and,

$$E = RT(\ln At + \gamma)$$

where, $p_{O\infty O}$: the activation energy distribution,

E : the mean activation energy at which annealing is occuring, and

γ : 0.577····

As concluded by Kimmel and Uhlmann (52), this is valid for both linear (n=1) and nonlinear (n≠1) distributed relaxation processes. By employing a frequency factor of $10^{7.44}$ sec^{-1} for PVC, which is based on other studies (51, 53, 54), the activation energy distribution of Figure 15 is shown in Figure 26. Apparently, a broad distribution in the activation energy spectra is observed when the final temperatures are far below T_g. In contrast, when the final temperatures are in the vicinity of T_g, the high energy portion of the distribution tends to decrease and results in the distribution narrowing sharply. In essence, this reflects both the nonlinear behavior and a distribution of activation energies or retardation times in the vicinity of T_g.

As combined with the isothermal volume contraction results obtained from hydrostatic weighing, it becomes apparent that densification or free volume diminishing in the glassy polymer takes place as a linear function of logarithmic aging time at the temperatures far below T_g. More specifically, at room temperature the intrinsic contraction behavior in a nonequilibrium glassy matrix of PVC can be suitably described by a single parameter model or the free volume theory.

Having concluded the studies concerning the diminishing free volume, we are now in a good position to examine the effects of the trapped free volume in the glassy matrix upon

its concomitant mechanical properties. This requires monitoring the subsequent physical properties under the same kind of thermal treatments. As shown in Figure 21, the concept of diminishing free volume in the glassy polymer has been revealed from the study of creep behavior by aging the same quenched specimen, under the same quenching conditions, at room temperature for various aging intervals. The most significant characteristic is that such curves can be superposed by shifting along the logarithmic time axis with a shift rate, μ, defined as (14)

$$\mu = - d \log a / d \log t_e$$

where, a is the shift factor and t_e the aging time. Accordingly, the aging effect on creep behavior shown in Figure 21 can be represented as $0.67 \log (t_e/t)$ where t_r is an arbitrary reference aging time, 9 minutes in this instance. In addition, nearly a linear shifting relationship is associated with the aging effect on the creep behavior. Obviously, this lends support to the conclusion resulting from volume contraction isotherms: a linear behavior characterizes the densification of quenched PVC specimens at room temperature. Further, Figure 22 clearly displays that the creep behavior is governed by the amount of excess free volume

trapped in the glassy matrix. Another mechanical property sensitive to free volume effects is stress-strain to failure shown in Figure 18 which reveals a transition from a general ductile behavior to brittle fracture as aging proceeds with time. Thus, the various experiments which have been carried out and described lead to a common conclusion: the excess free volume content trapped in glassy PVC due to rapid quenching is small, but it directly and strongly affects the concomitant mechanical properties.

CONCLUSIONS

Using the techniques of hydrostatic weighing and volume dilatometry, specific volume changes in PVC film specimens, due to rapid quenching through the glass transition, have been studied. Both results clearly demonstrate the more severe the quench, the greater is the departure from equilibrium volume or the greater is the free volume content. Further, aging of relaxing molecular rearrangements, based on the studies of phenomenological events, takes place as a linear function of logarithmic aging time at temperatures far below T_g. In the vicinity of T_g, however, either distributions of retardation times or activation energy spectra are required to describe the nonequilibrium glassy behaviors.

Studies of concomitant mechanical properties monitored by tensile creep strongly reveal the dependence of the creep behavior on the trapped free volume content. Experimental results distinctly demonstrate that the phenomena of aging and quenching are essentially thermoreversible. Further, a linear relationship of log (shift factor) vs. log (aging time) is observed from investigating the creep behaviors of PVC film specimens at various aging intervals after quenching.

This observation strongly corroborates the linear behavior of diminishing free volume mentioned earlier. In addition, a transition from a general ductile behavior to brittle fracture, as aging proceeds with time, is observed from the study of stress-strain to failure. In view of these facts, it is evident that the volume changes in the glassy matrix of PVC due to rapid quenching and subsequent aging are relatively small, but directly and strongly affect the concomitant mechanical properties.

FUTURE WORK

Since positive results have been obtained from pnenomenological approaches, future studies regarding the rapid quenching effects in glassy polymers will be continued by means of hydrostatic weighing and volume dilatometry. Based on this study, it is hoped to gain further insight into the non-equilibrium behaviors of some glassy polymers. The range of work will be expanded from the vicinity of T_g, to the lower transition region, for instance, T_β. In order to predict the changes in material properties or further utilize the benefits of rapid quenching effects for glassy polymers as engineering materials, creep testing or possibly dynamic mechanical testing will be used to reflect the molecular mobility of quenched or aged glassy polymers. Although various degrees of success have been or will be achieved by utilizing the abovementioned approaches, it is hoped that a correlationship between molecular motion and observed macroscopic properties can be made. In this respect, high-resolution NMR has recently been recognized as a powerful tool for studying molecular structure (55, 56, 57, 58). Accordingly, NMR will be applied in an attempt to obtain direct evidence revealing

the molecular motion changes in solid glassy polymers due to quenching and subsequent aging effects. The frame work of this research, thus, is summarized on the following page.

ACKNOWLEDGEMENT

This work was supported by the National Aeronautics and Space Administration Headquarters, Washington, D.C., Materials Processing in Space Division.

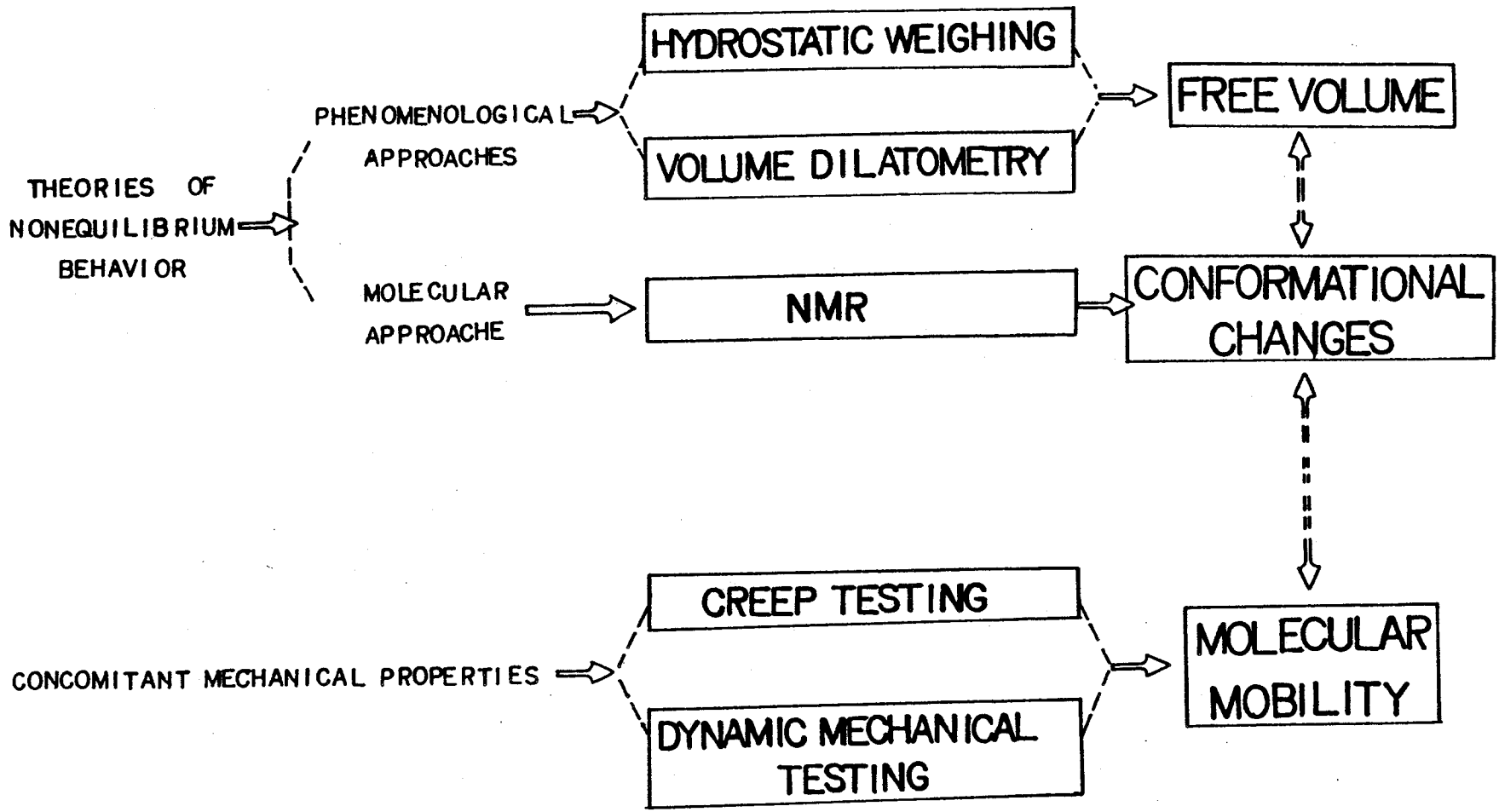
THEORIES OF NONEQUILIBRIUM BEHAVIOR
PHENOMENOLOGICAL APPROACHES
HYDROSTATIC WEIGHING
VOLUME DILATOMETRY
FREE VOLUME
MOLECULAR APPROACHE
NMR
CONFORMATIONAL CHANGES
CONCOMITANT MECHANICAL PROPERTIES
CREEP TESTING
DYNAMIC MECHANICAL TESTING
MOLECULAR MOBILITY

FIGURE CAPTIONS

Figure 1. Schematic diagram showing the specimen wrapped in aluminum foil and copper sheet with a thermocouple inserted into the sandwich for temperature reading during quenching and annealing.

Figure 2. Idealized cooling rates* of ice-water quenching and air cooling from 100^{o}C (* monitored from thermocouple inserted in the sandwich structure in Figure 1).

Figure 3. Apparatus for hydrostatic weighing.

Figure 4. Apparatus for suspension wire treatment.

Figure 5. Precision thermoregulator.

Figure 6. Apparatus for mercury filling.

Figure 7. Apparatus for dilatometry measurement.

Figure 8. Apparatus for non-contact creep measurement.

Figure 9. Weight loss and density measurements of solvent-cast films subjected to various annealing cycles.

Figure 10. Weight loss and density measurements of melt-molded films subjected to various annealing cycles.

Figure 11. Effect of quenching rates on the specific volume and volume contraction behavior of PVC melt-molded film (Geon 128) at 20°C measured by hydrostatic weighing. Film was subjected to ice water quenching or air cooling from 100°C.

Figure 12. Effect of quenching PVC film specimen (Geon 121), from various initial temperatures to ice water, on the specific volume and volume contraction behavior at 20°C.

Figure 13. Specific volumes at equilibrium state for PVC measured by dilatometer from 78°C to 130°C.

Figure 14. Isothermal volume contractions of PVC, quenched from equilibrium at 99°C to various final temperatures far below T_g.

Figure 15. Isothermal volume contractions of PVC, from equilibrium at 99°C to various final temperature in the vicinity of T_g.

Figure 16. Isochronal specific volume vs. temperature for PVC showing glass transition temperature dependence upon aging time.

Figure 17. Effects of quenching PVC from various initial temperatures to the same aging temperature, 20°C, on the trapped free volume and volume contractions (by dilatometer).

Figure 18. Tensile stress-strain to failure properties for quenched PVC film specimens against aging time at room temperature.

Figure 19. Proof testing of creep apparatus shown in Figure 8 with aluminum foil, and comparative creep behavior of PVC film specimens.

Figure 20. Thermoreversibility of quenching.

Figure 21. Aging effects on creep behavior of quenched PVC film.

Figure 22. Effect of quenching from various initial temperatures above T_g to ice water on the creep behavior of PVC at the same aging interval.

Figure 23. T_g of PVC vs. log aging time.

Figure 24. Experimental plots of log τ_{eff} vs. δ for PVC quenched from the same temperature to various aging temperature.

Figure 25. Experimental plots of log τ_{eff} vs. δ for PVC quenched from various temperatures to the same aging temperature.

Figure 26. Activation energy distribution for PVC quenched from the same temperature to various aging temperatures.

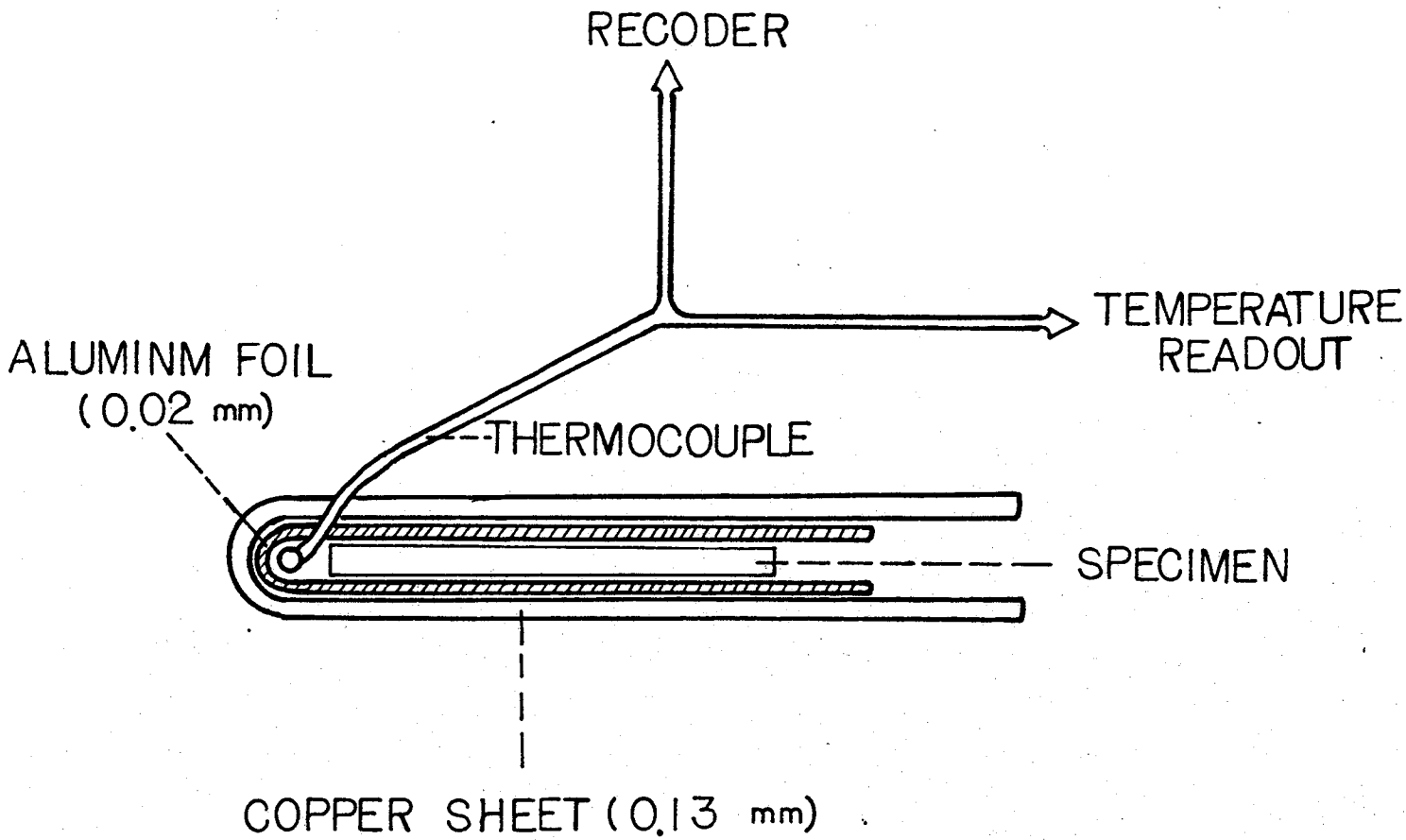
RECODER
TEMPERATURE
READOUT
ALUMINM FOIL
(0.02 mm)
THERMOCOUPLE
SPECIMEN
COPPER SHEET (0.13 mm)

FIG. 1

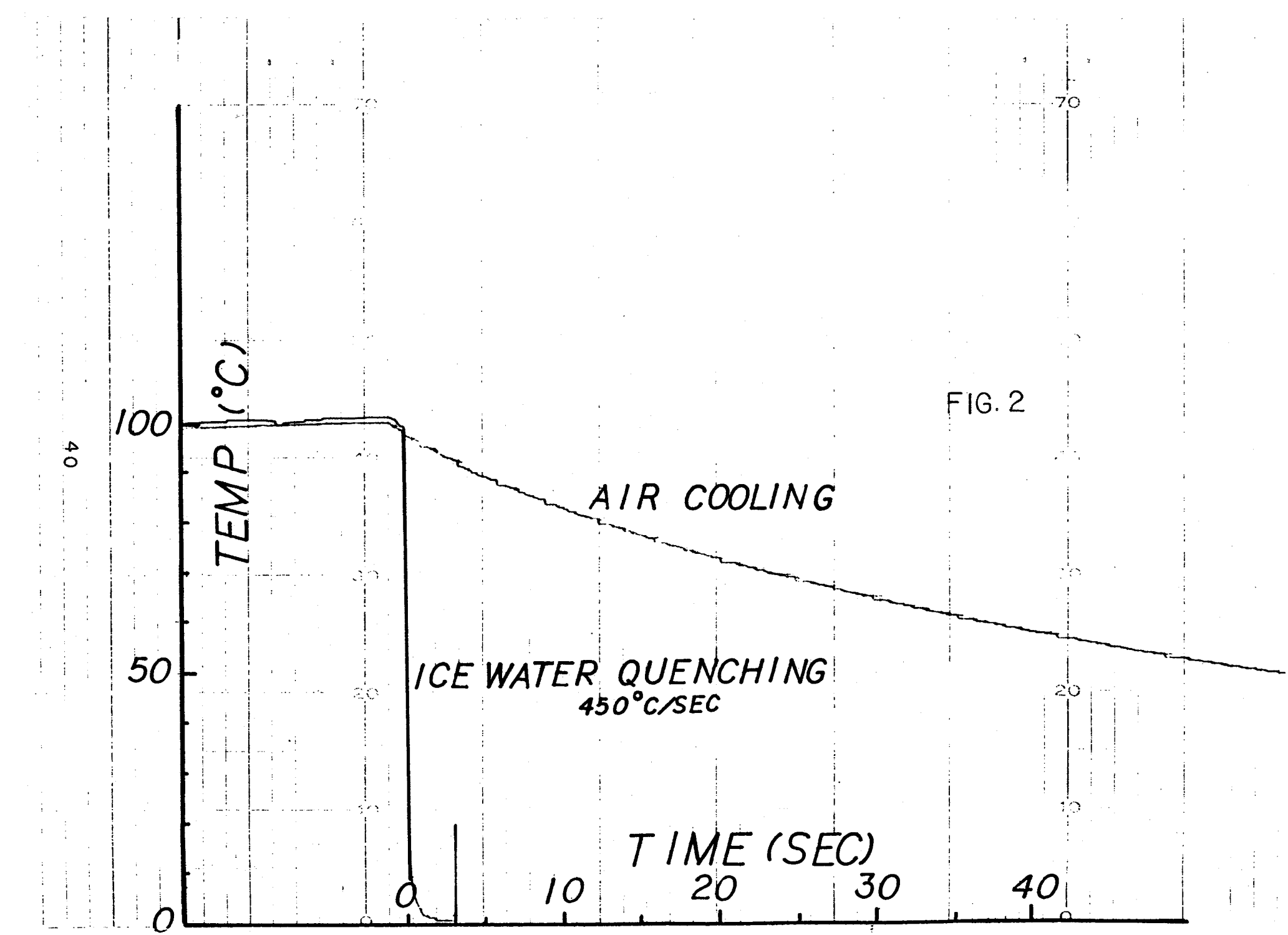

FIG. 2

CONTROLS CORPORATION BUFFALO, NEW YORK PRINTED IN U.S.A.

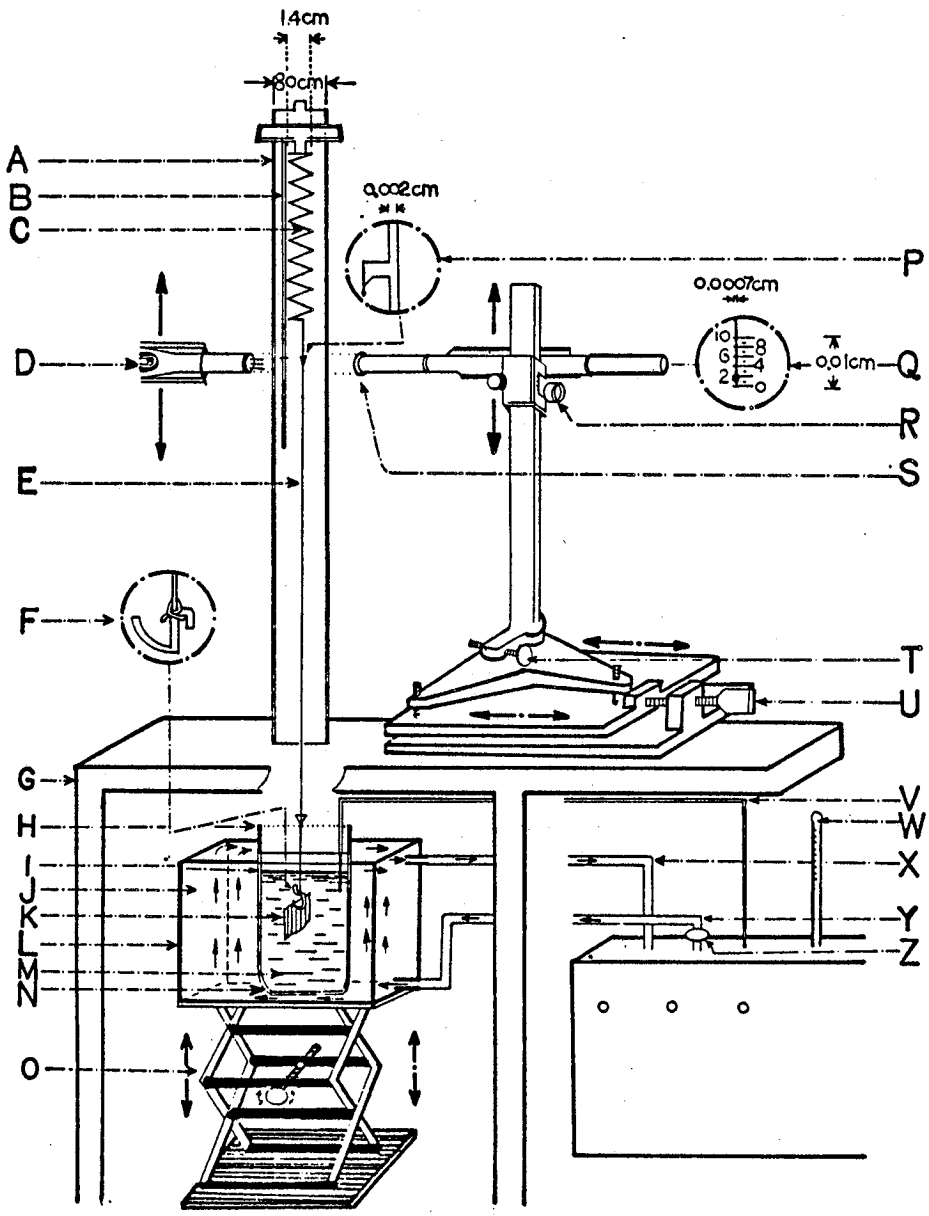

Figure 3

HYDROSTATIC BALANCE

maximum load: 60 mg

sensitivity : 0.0001 cm^3/g or better

A: Pyrex glass tube (80 cm diameter)

B: Reference scale

C: Helical spring made of 0.011-cm tungsten wire, or 0.01-cm music wire with 1.4 cm coil diameter

D: Intense light

E: Optical fiber (0.002 diameter)

F: Tungsten-wire-hook tied by optical fiber (no adhesive)

G: Closed system to prevent air flow

H: Constant depth marker for immersion wire

I: Immersion liquid level marker

J: Constant temperature bath

K: Specimen

L: Visible container for constant temperature fluid

M: Immersion liquid (degassed distilled water)

N: Visible container for immersion liquid

O: Jack

P: Coarse target

Q: Fine target (marker with 0.0007 cm diameter)

R: Height reading

S: Light filter

T: Horizontal angle adjuster

U: Focus adjuster

V: Immersion liquid thermal couple

W: Bath temperature

X: Constant temperature bath outlet

Y: Constant temperature bath inlet

Z: Flow valve

Figure 3 A detailed diagrammatic view of density device and notes.

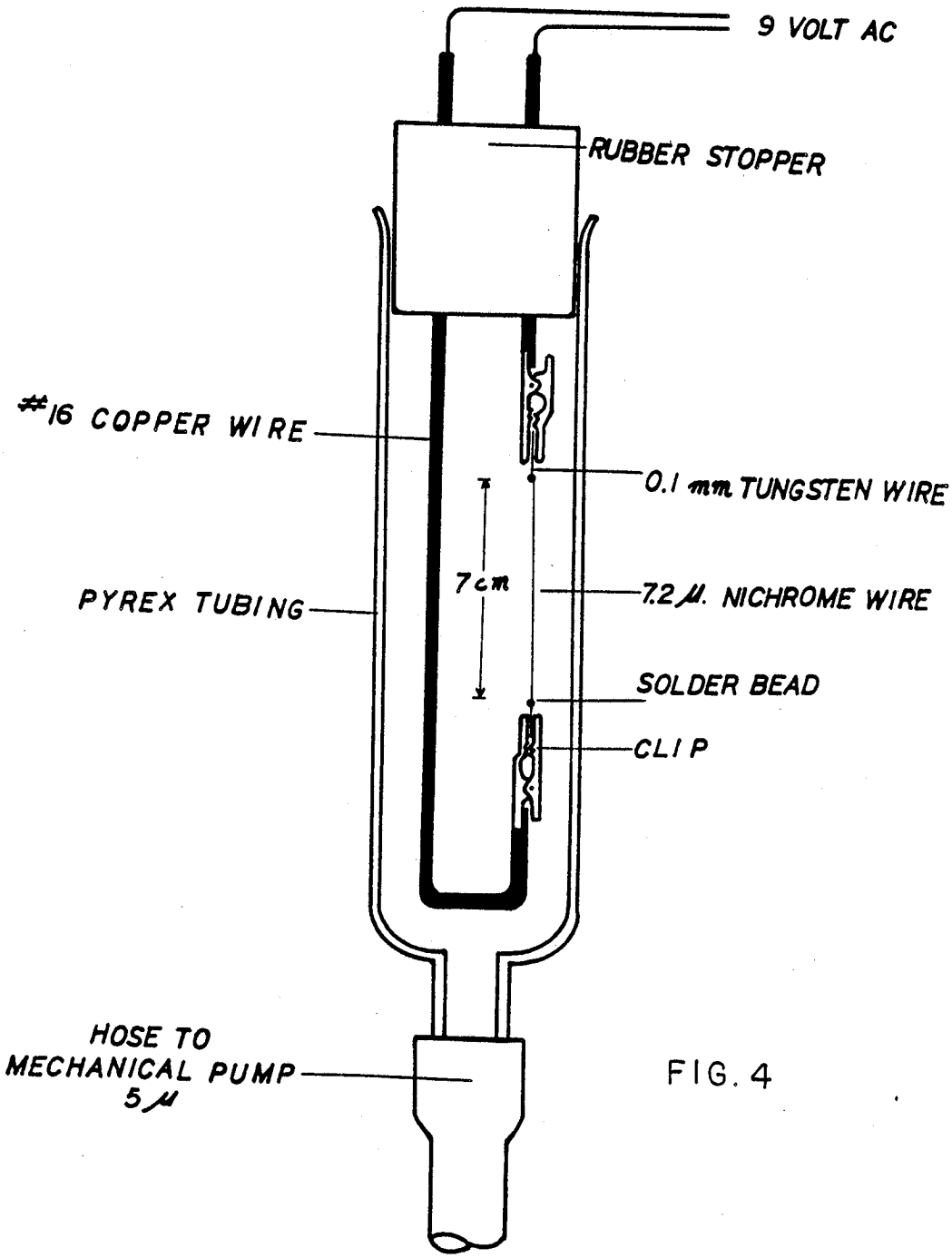
9 VOLT AC
RUBBER STOPPER
#16 COPPER WIRE
0.1 mm TUNGSTEN WIRE
7 cm
PYREX TUBING
7.2 μ. NICHROME WIRE
SOLDER BEAD
CLIP
HOSE TO
MECHANICAL PUMP
5 μ

FIG. 4

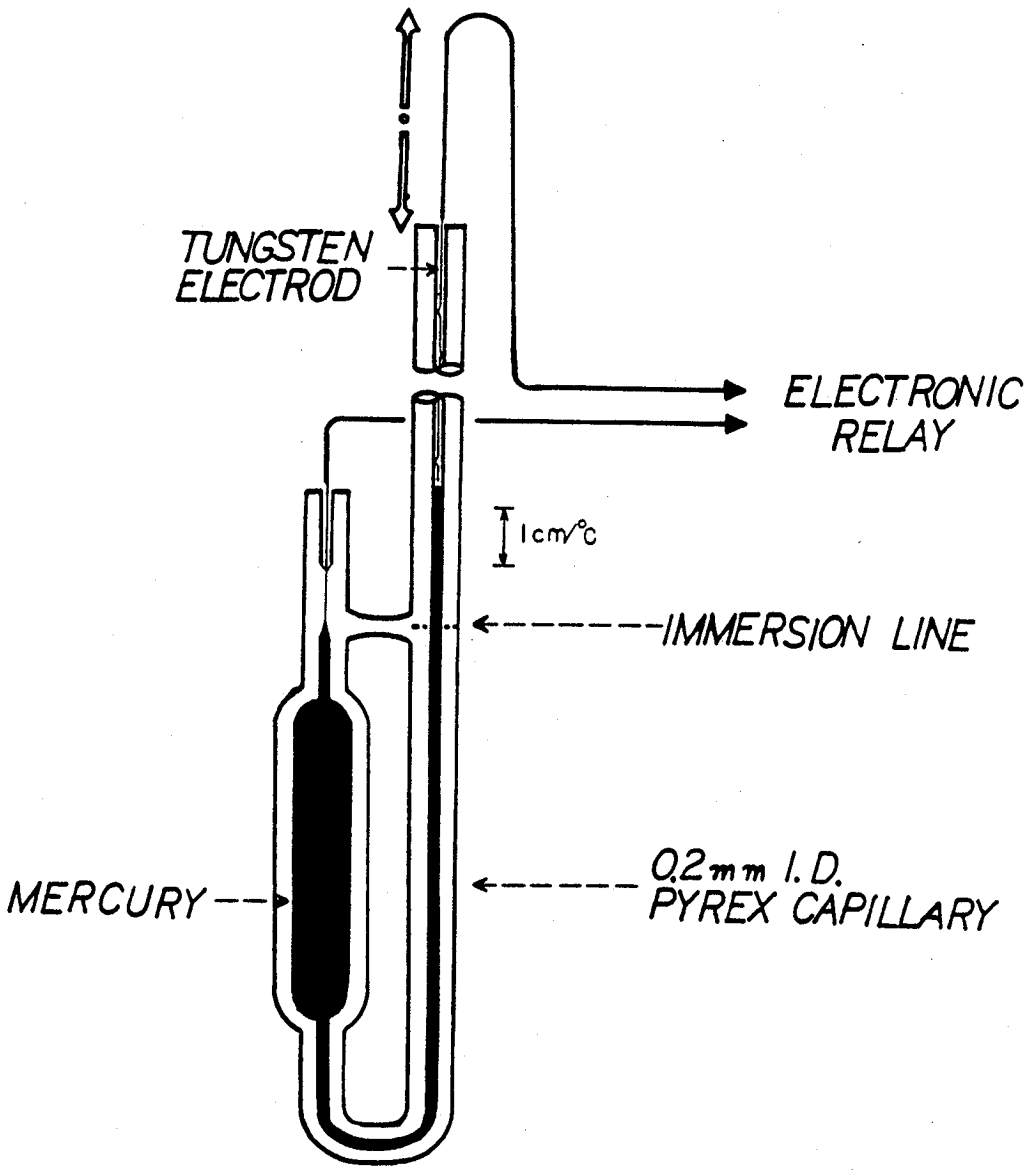

FIG. 5

PRECISION THERMOREGULATOR

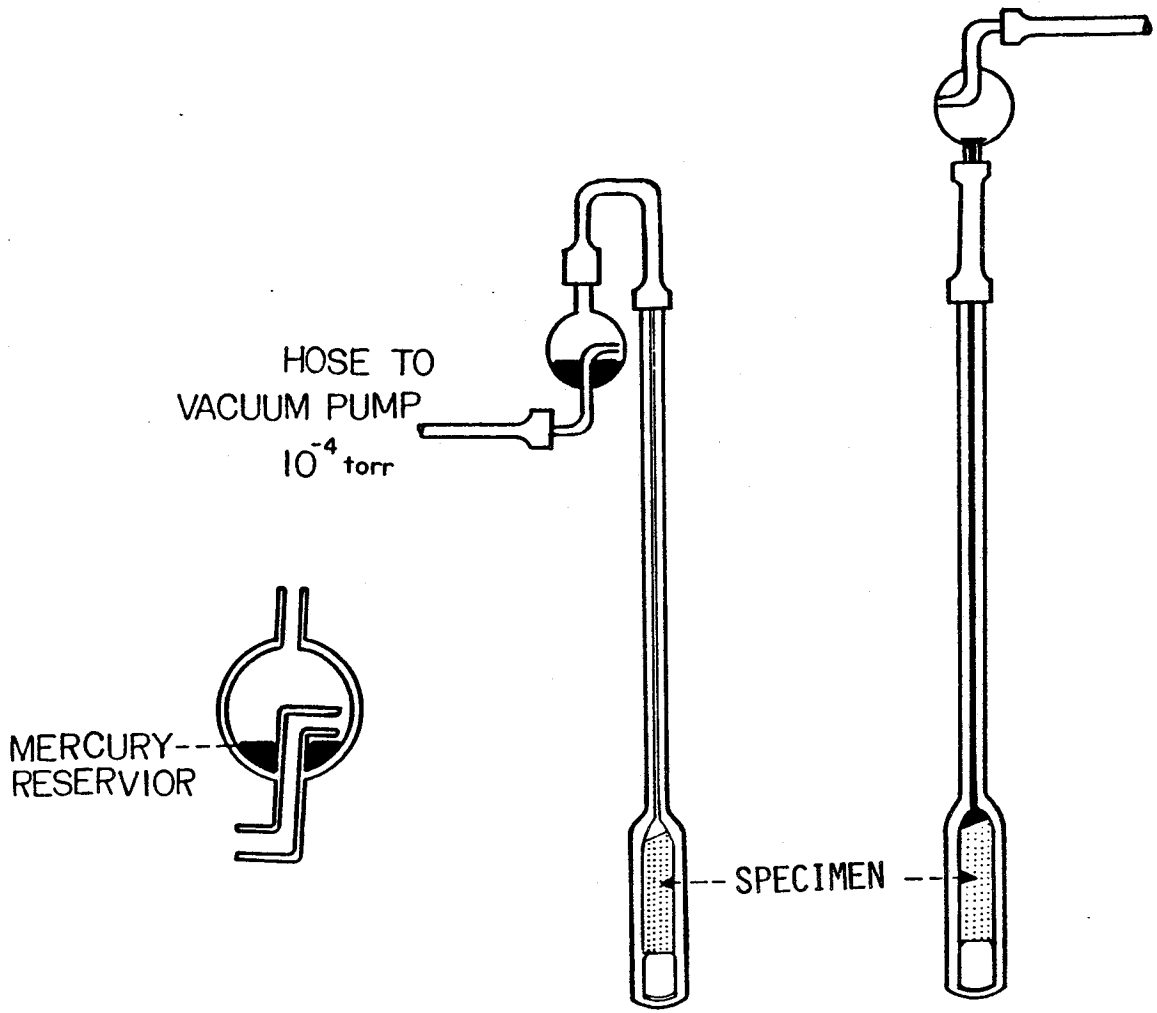

FIG. 6

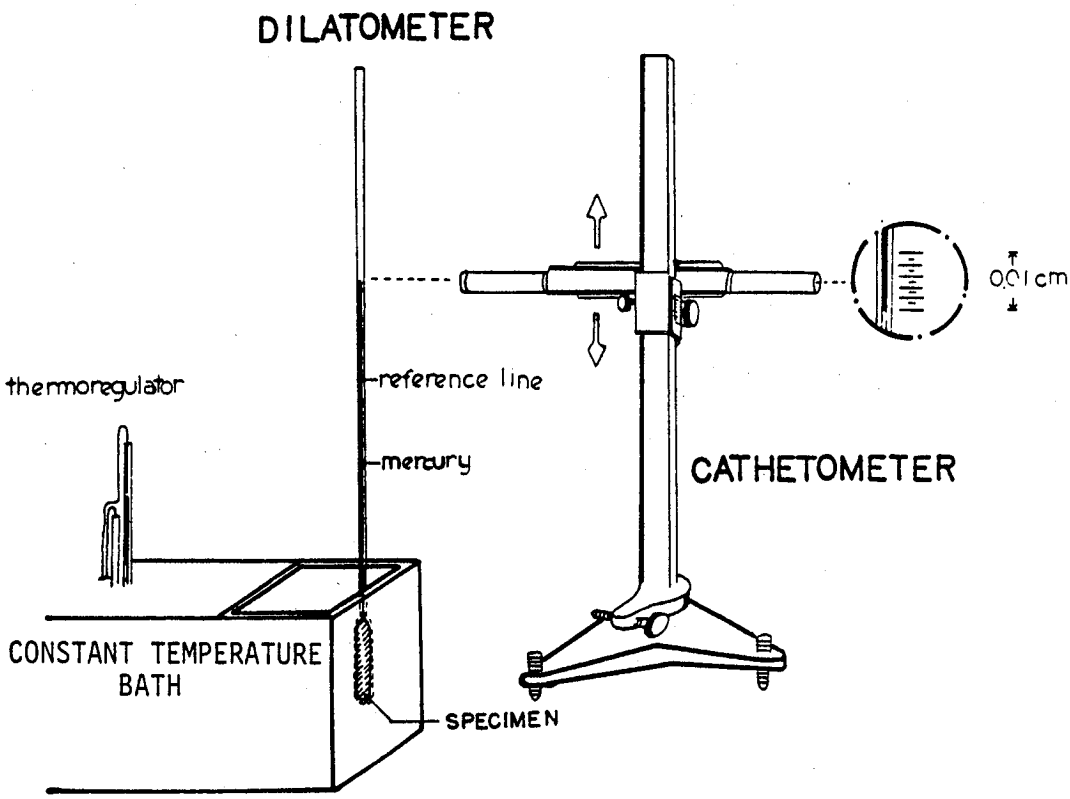

DILATOMETRY MEASUREMENT

FIG. 7

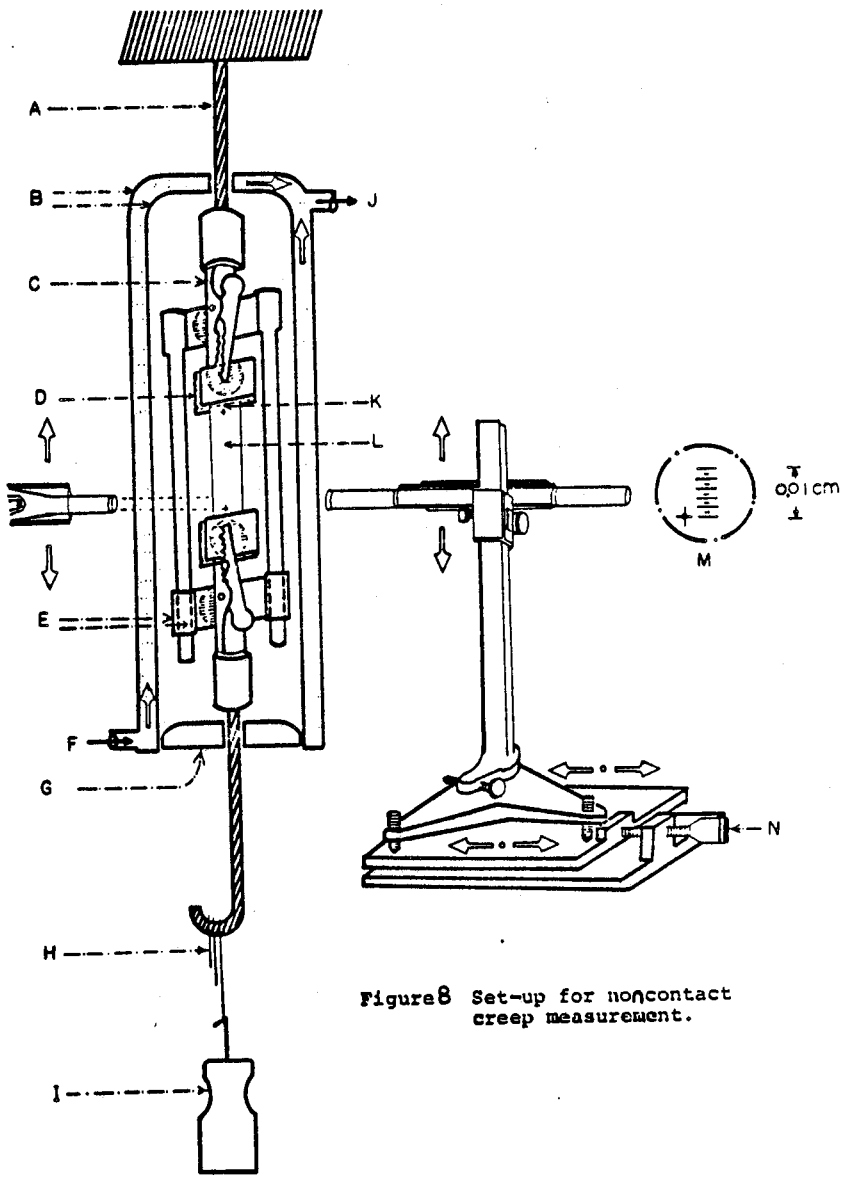

Figure 8 Set-up for noncontact creep measurement.

A: No. 13 Copper wire

B: Pyrex glass

C: Mueller clip

D: Aluminum sheet (0.05 cm thick)

E: Pyrex tubing and Pyrex rod

F: Inlet of constant temperature water

G: Rubber stopper

H: Fine load

I: Coarse load

J: Outlet of water circulation

K: No. 220 Sandpaper

L: Sample with two targets

M: Fine target (resolution: 0.0004 cm)

N: Focus adjuster

Figure 8 A detailed diagrammatic view of creep tester and its notes.

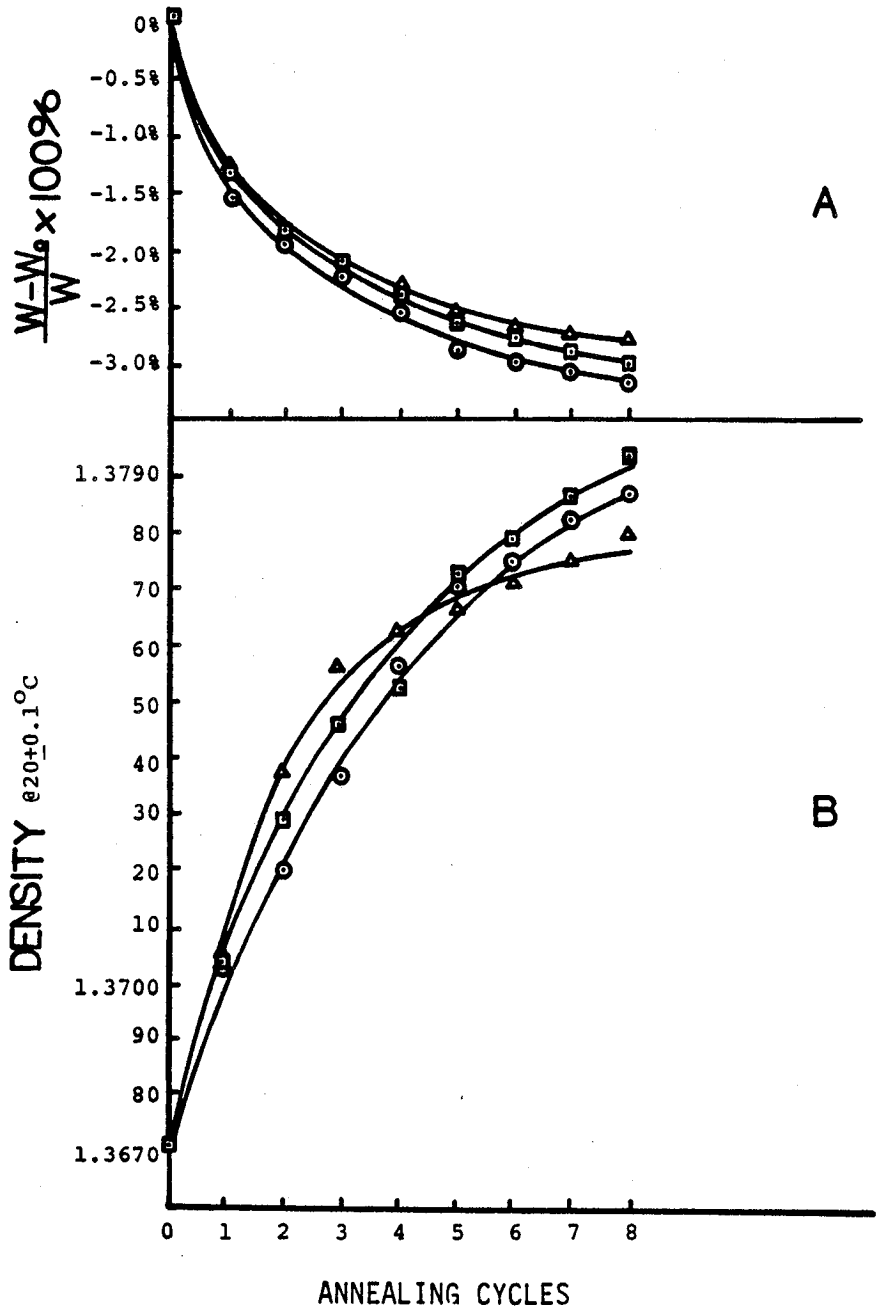

Figure 9 Effects of various annealing cycles at constant annealing temperature (T_{max}=140°C, t_{max}=3 min) on (a) weight loss, and (b) corresponding densities for solvent-cast films (Geon 121).

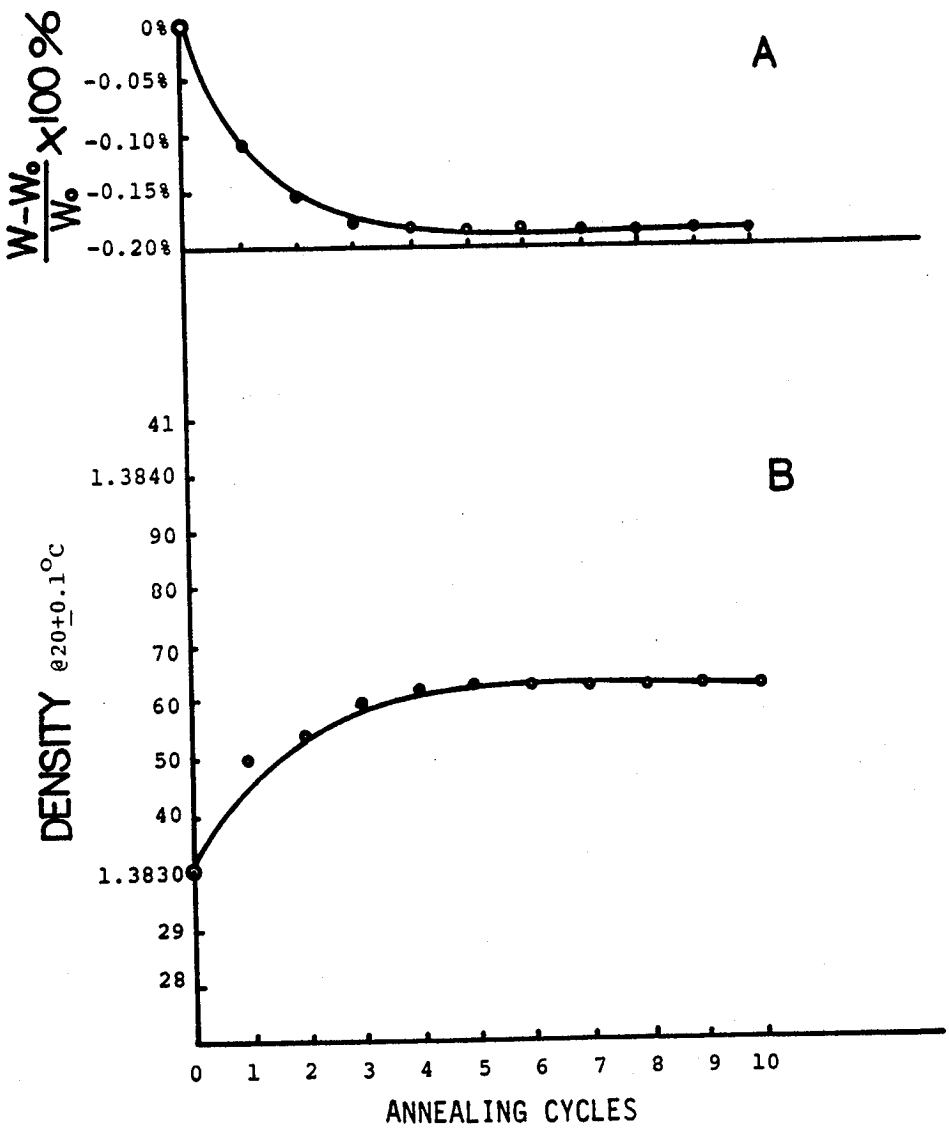

Figure 10 Effects of various annealing cycles at constant annealing temperature (T_{max}=145°C, t_{max}=3 min) on (a) weight loss, and (b) corresponsing densities for melt-molded PVC film (Geon 121).

FIG. 11

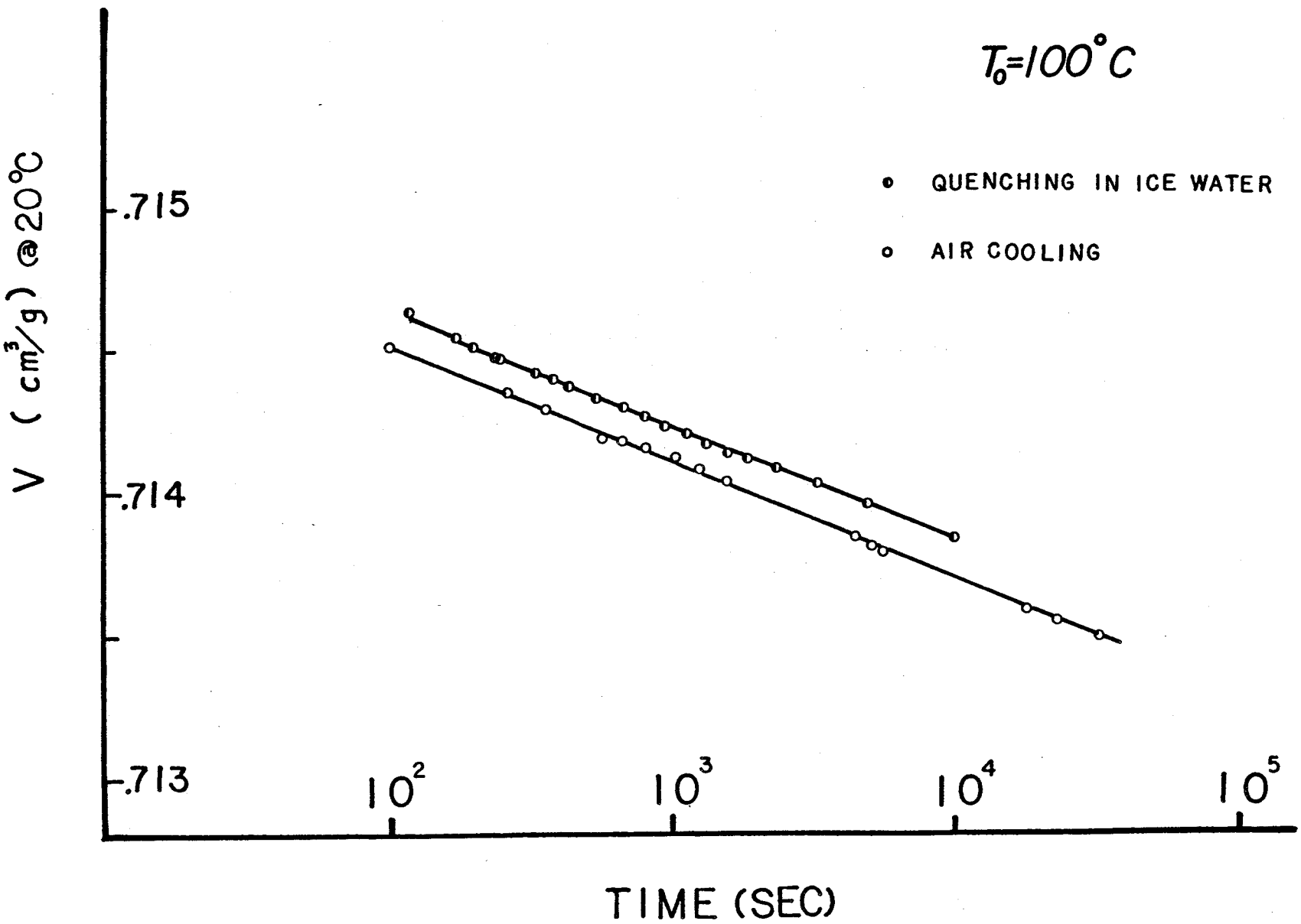
T_0=100°C
QUENCHING IN ICE WATER
AIR COOLING
V (cm³/g) @20°C
.715
.714
.713
10^2
10^3
10^4
10^5
TIME (SEC)

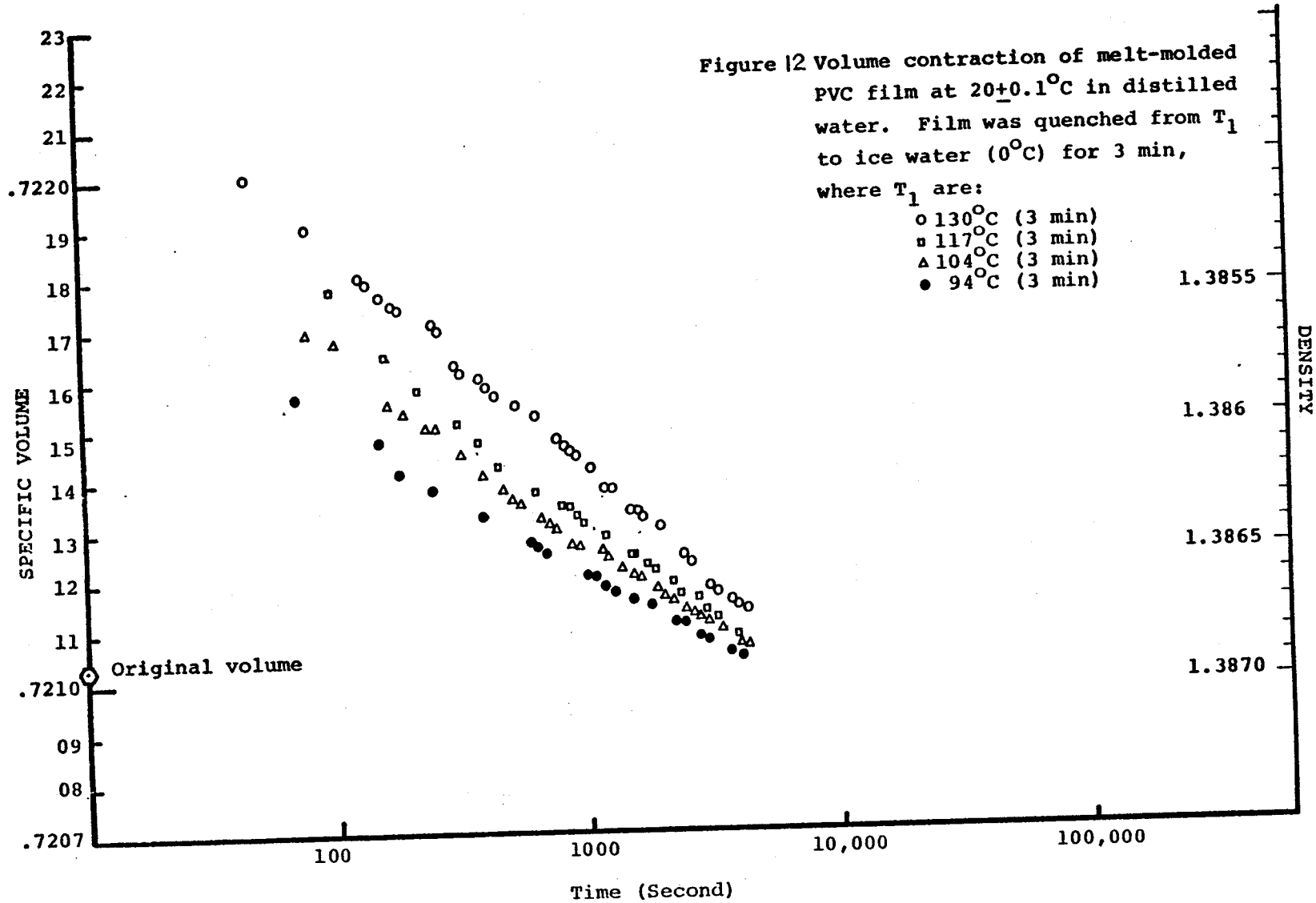

Figure 12 Volume contraction of melt-molded PVC film at 20±0.1°C in distilled water. Film was quenched from T_1 to ice water (0°C) for 3 min, where T_1 are:

- o 130°C (3 min)
- ▫ 117°C (3 min)
- △ 104°C (3 min)
- ● 94°C (3 min)

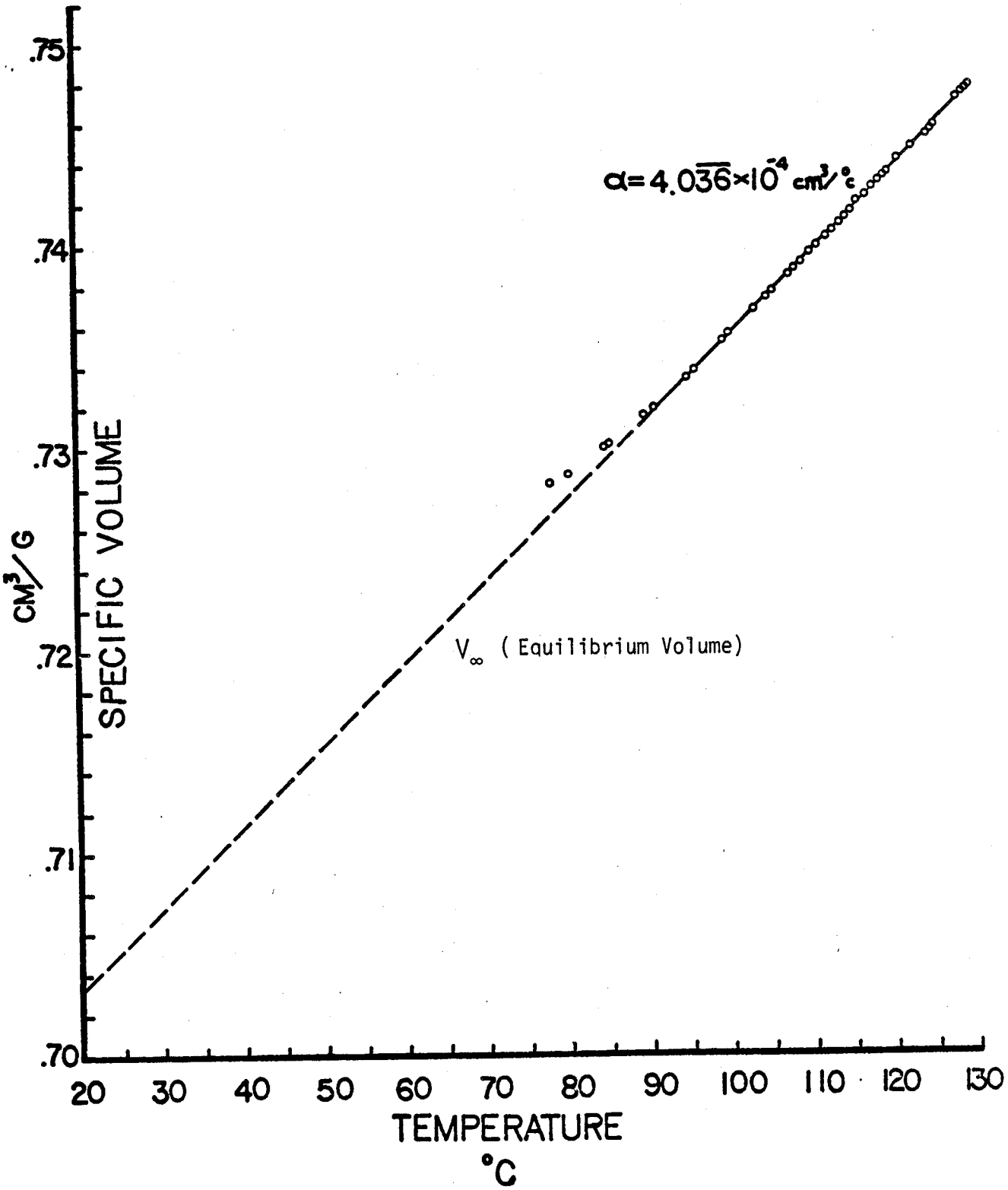
.75
.74
.73
.72
.71
.70
SPECIFIC VOLUME
CM³/G
α=4.036×10⁻⁴ cm³/°c
V∞ (Equilibrium Volume)
20
30
40
50
60
70
80
90
100
110
120
130
TEMPERATURE
°C

FIG. 13

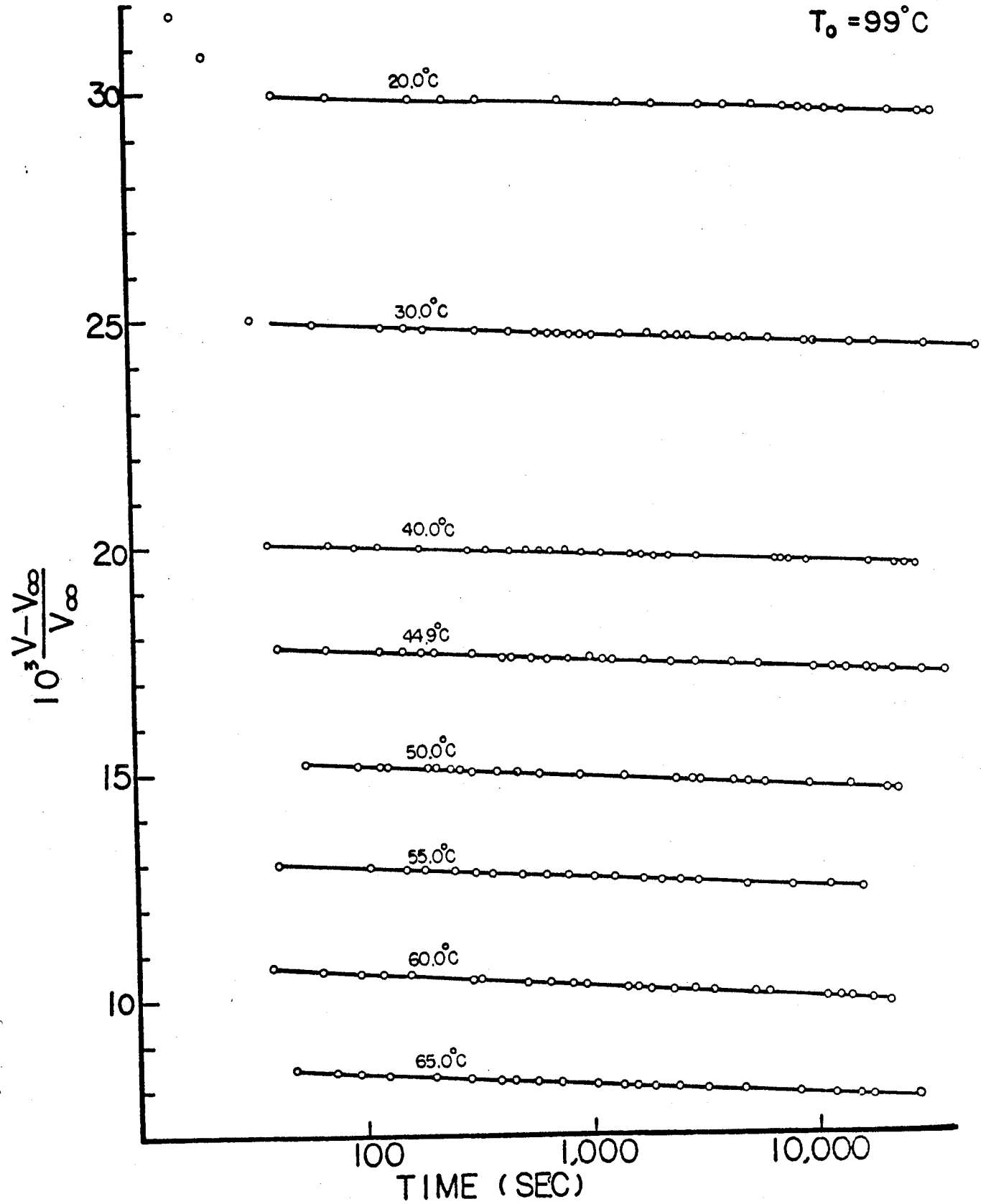
T_0 = 99°C
20.0°C
30.0°C
40.0°C
44.9°C
50.0°C
55.0°C
60.0°C
65.0°C
30
25
20
15
10
$10^3 \frac{V - V_\infty}{V_\infty}$
100
1,000
10,000
TIME (SEC)

FIG. 14

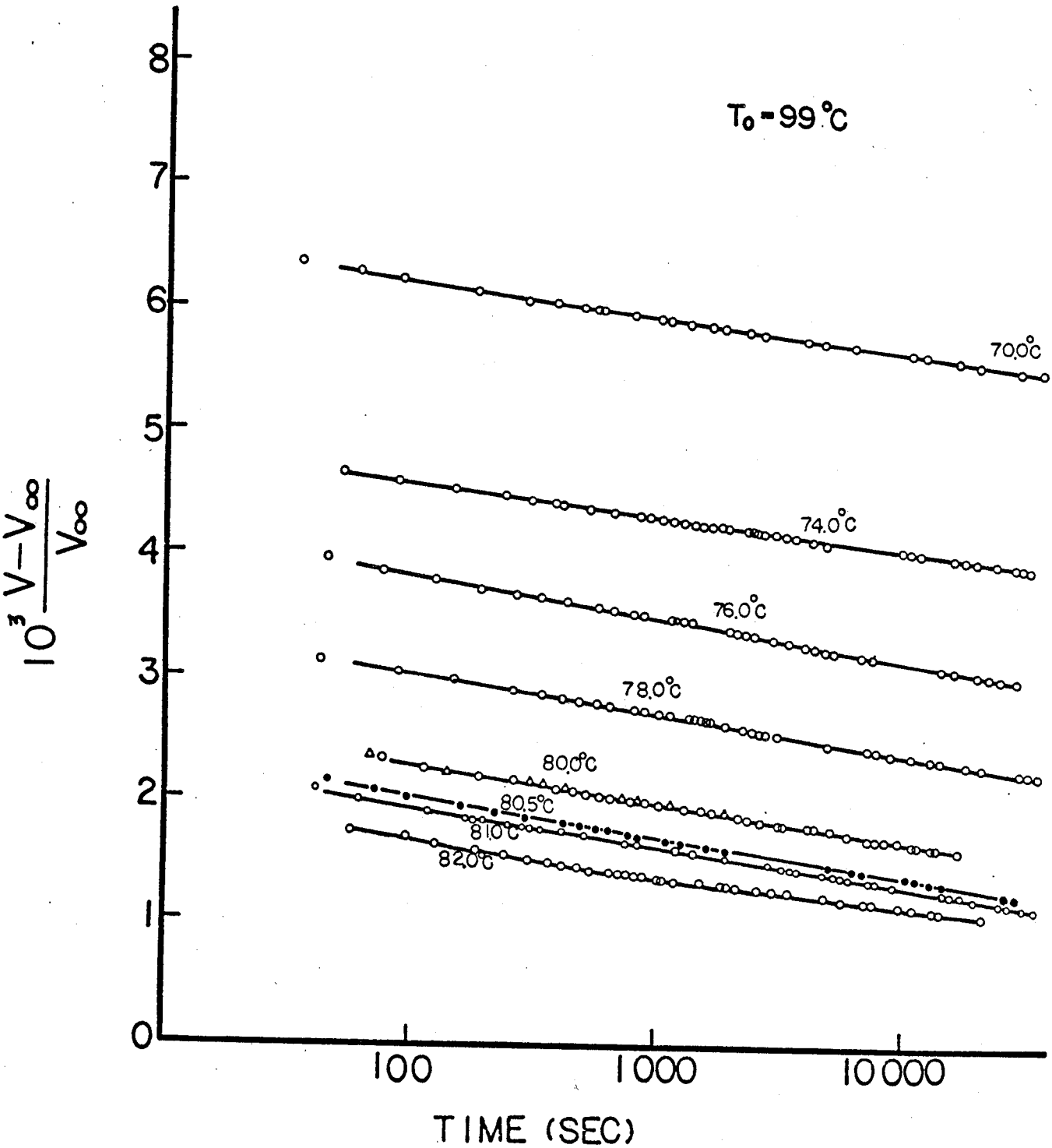
$T_0 = 99°C$
70.0°C
74.0°C
76.0°C
78.0°C
80.0°C
80.5°C
81.0°C
82.0°C
$10^3 \frac{V - V_\infty}{V_\infty}$
TIME (SEC)
0
1
2
3
4
5
6
7
8
100
1000
10000

FIG. 15

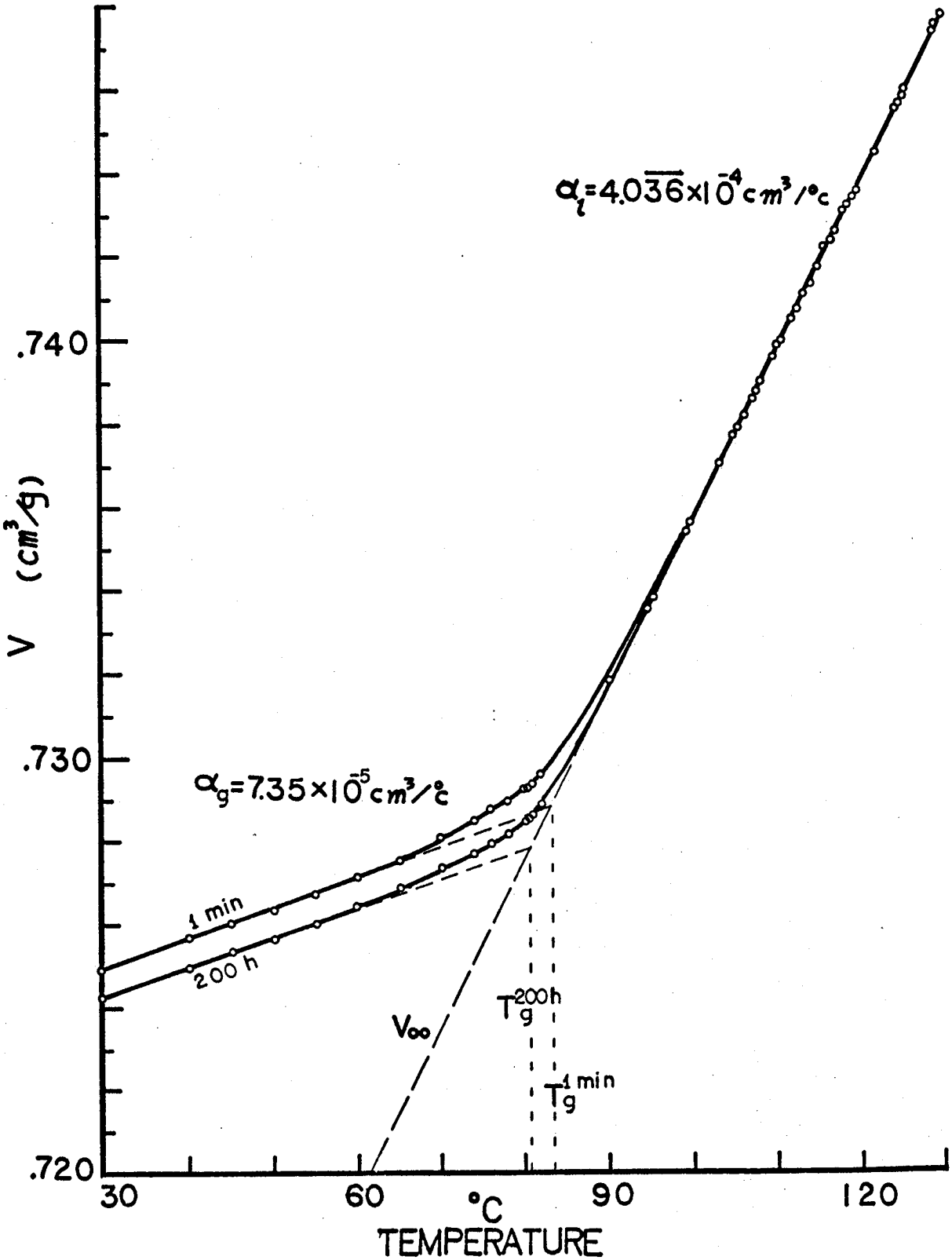
$\alpha_l = 4.036 \times 10^{-4}$ cm³/°c
.740
.730
.720
V (cm³/g)
$\alpha_g = 7.35 \times 10^{-5}$ cm³/°c
1 min
200 h
V_∞
T_g^{200h}
$T_g^{1\,min}$
30
60
°C
90
120
TEMPERATURE

FIG. 16

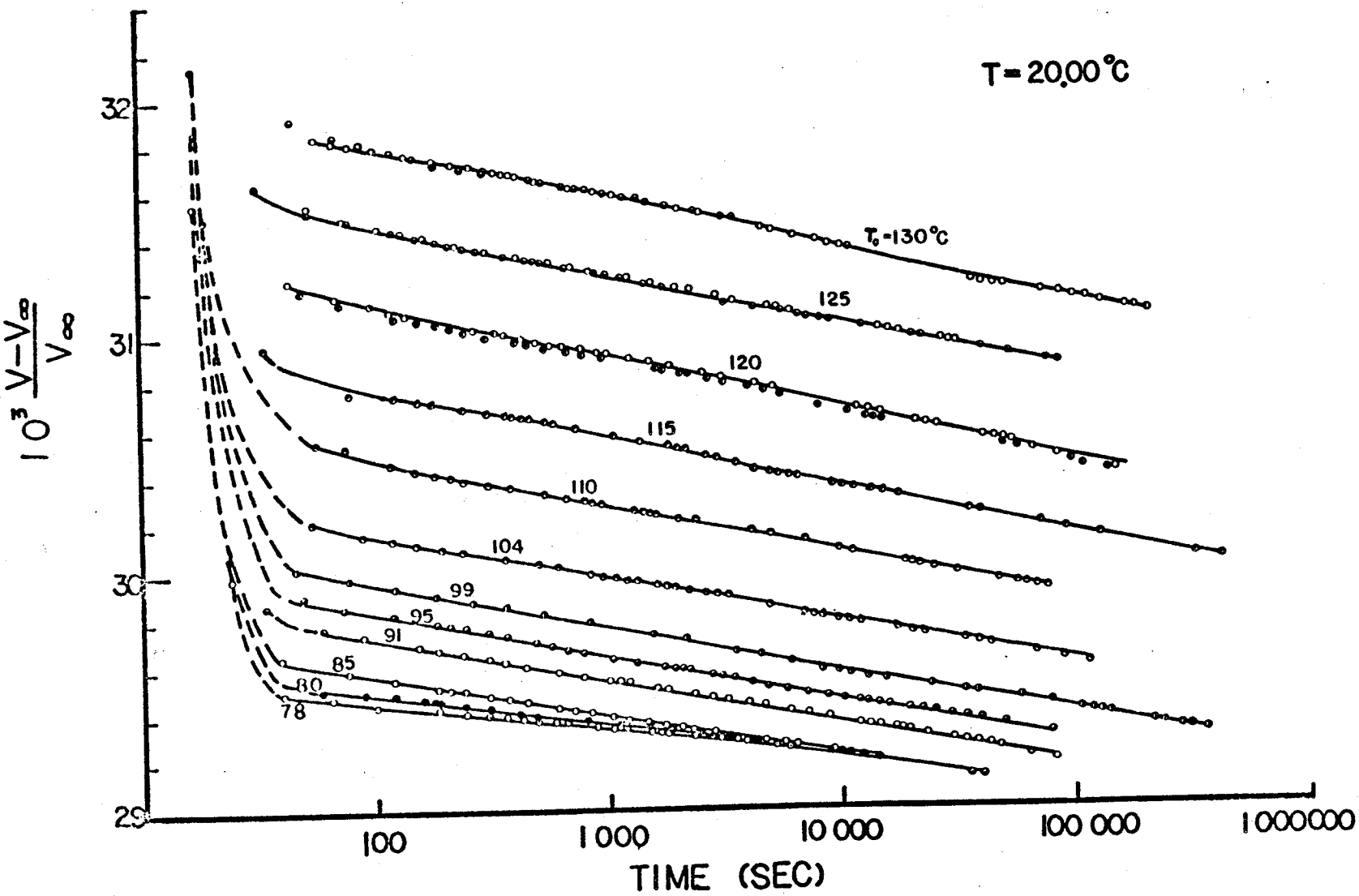
T = 20,00 °C
$10^3 \frac{V-V_8}{V_8}$
32
31
30
29
T_0 = 130 °C
125
120
115
110
104
99
95
91
85
80
78
100
1 000
10 000
100 000
1000000
TIME (SEC)

FIG. 17

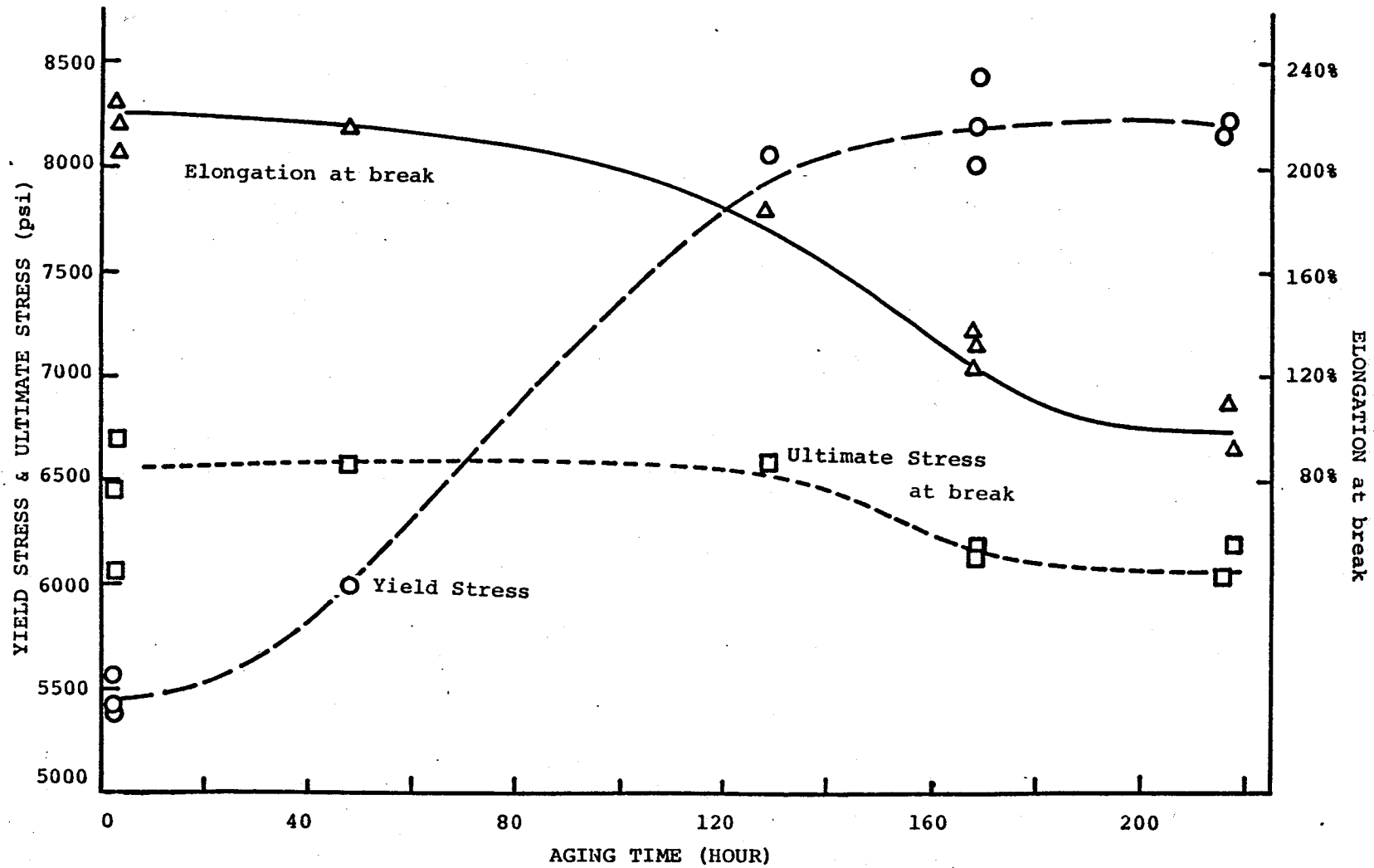

Figure 18 Tensile stress-strain properties of quenched PVC films (solvent-cast) against aging time at room temperature. Films were quenched in liquid Nitrogen from 118°C (t_{max}=3 min).

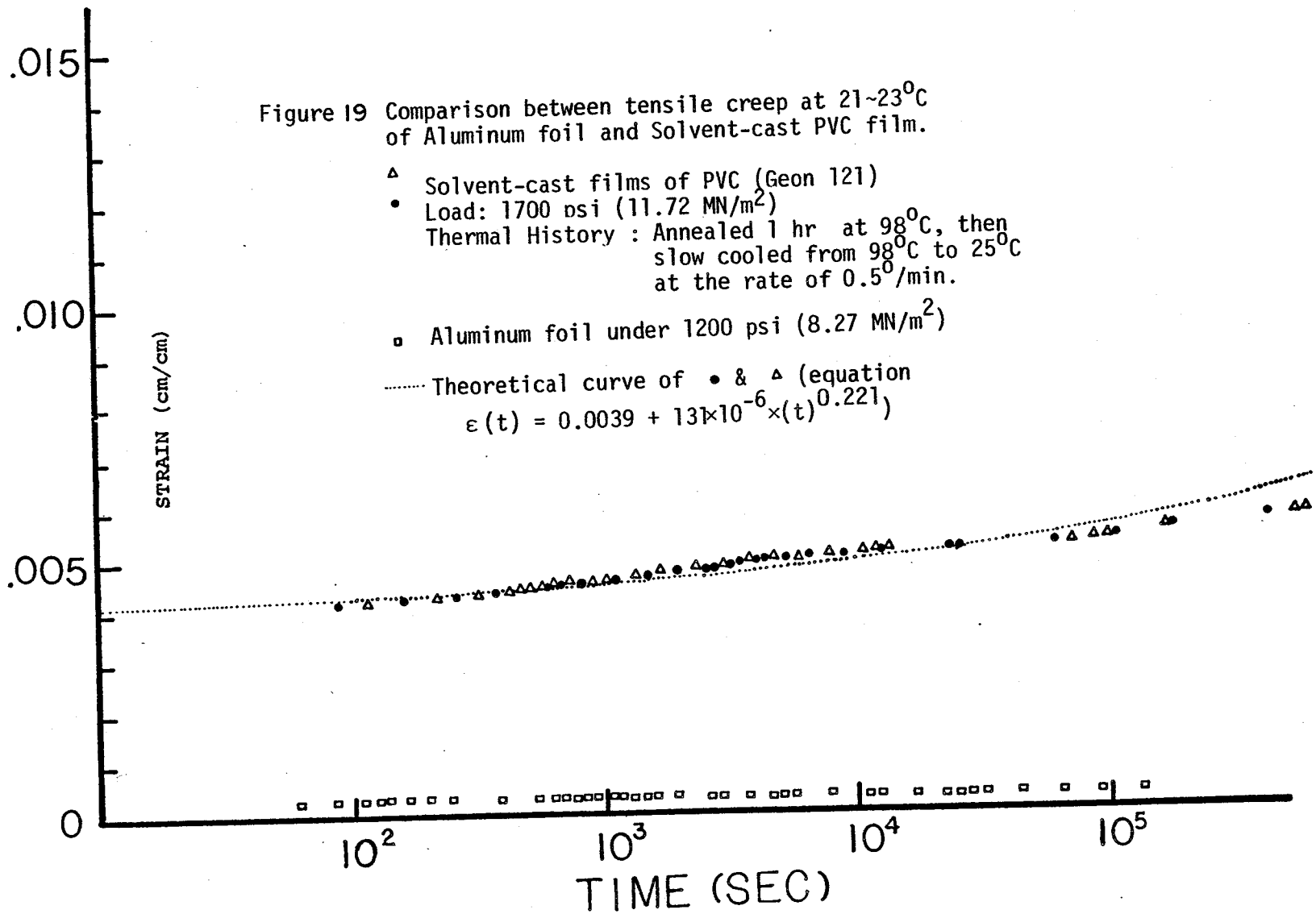

Figure 19 Comparison between tensile creep at 21~23°C of Aluminum foil and Solvent-cast PVC film.

△ Solvent-cast films of PVC (Geon 121)
• Load: 1700 psi (11.72 MN/m^2)
Thermal History : Annealed 1 hr at 98°C, then slow cooled from 98°C to 25°C at the rate of 0.5°/min.

▫ Aluminum foil under 1200 psi (8.27 MN/m^2)

····· Theoretical curve of • & △ (equation

$$\varepsilon(t) = 0.0039 + 131\times10^{-6}\times(t)^{0.221})$$

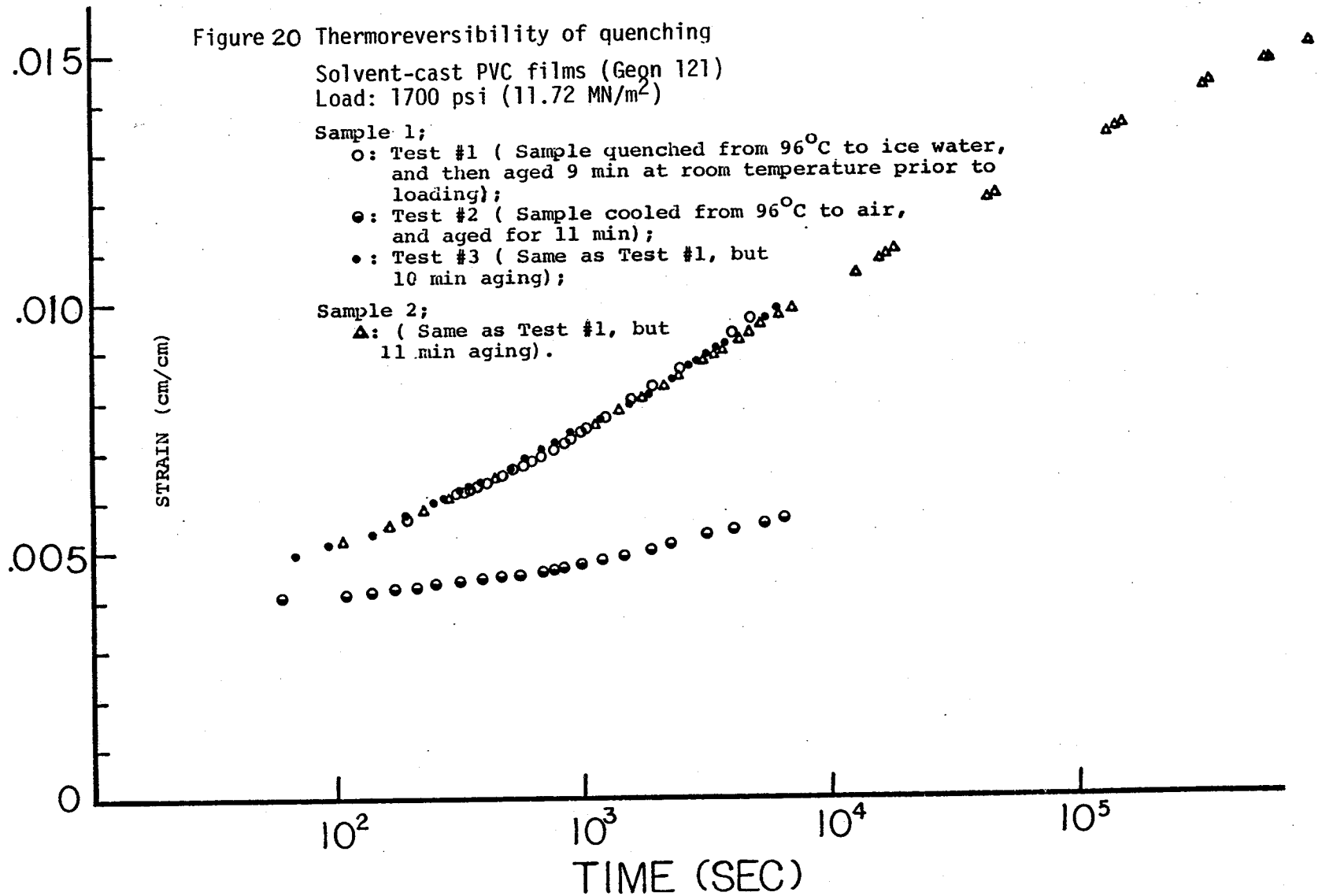

Figure 20 Thermoreversibility of quenching

Solvent-cast PVC films (Geon 121)
Load: 1700 psi (11.72 MN/m^2)

Sample 1;
- o: Test #1 (Sample quenched from 96°C to ice water, and then aged 9 min at room temperature prior to loading);
- ⊖: Test #2 (Sample cooled from 96°C to air, and aged for 11 min);
- •: Test #3 (Same as Test #1, but 10 min aging);

Sample 2;
- Δ: (Same as Test #1, but 11 min aging).

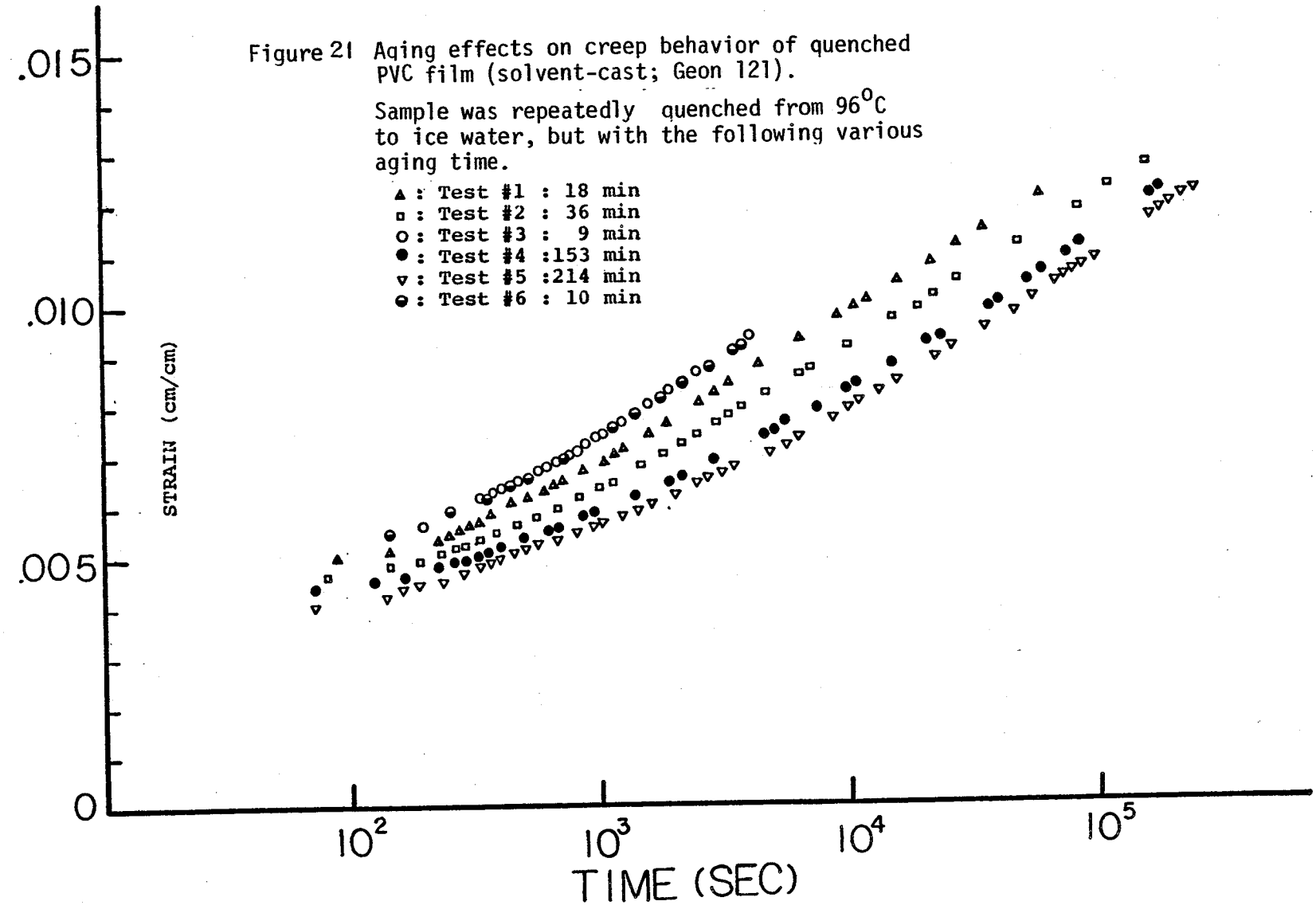

Figure 21 Aging effects on creep behavior of quenched PVC film (solvent-cast; Geon 121).

Sample was repeatedly quenched from 96°C to ice water, but with the following various aging time.

▲ : Test #1 : 18 min
▫ : Test #2 : 36 min
○ : Test #3 : 9 min
● : Test #4 : 153 min
▽ : Test #5 : 214 min
⊖ : Test #6 : 10 min

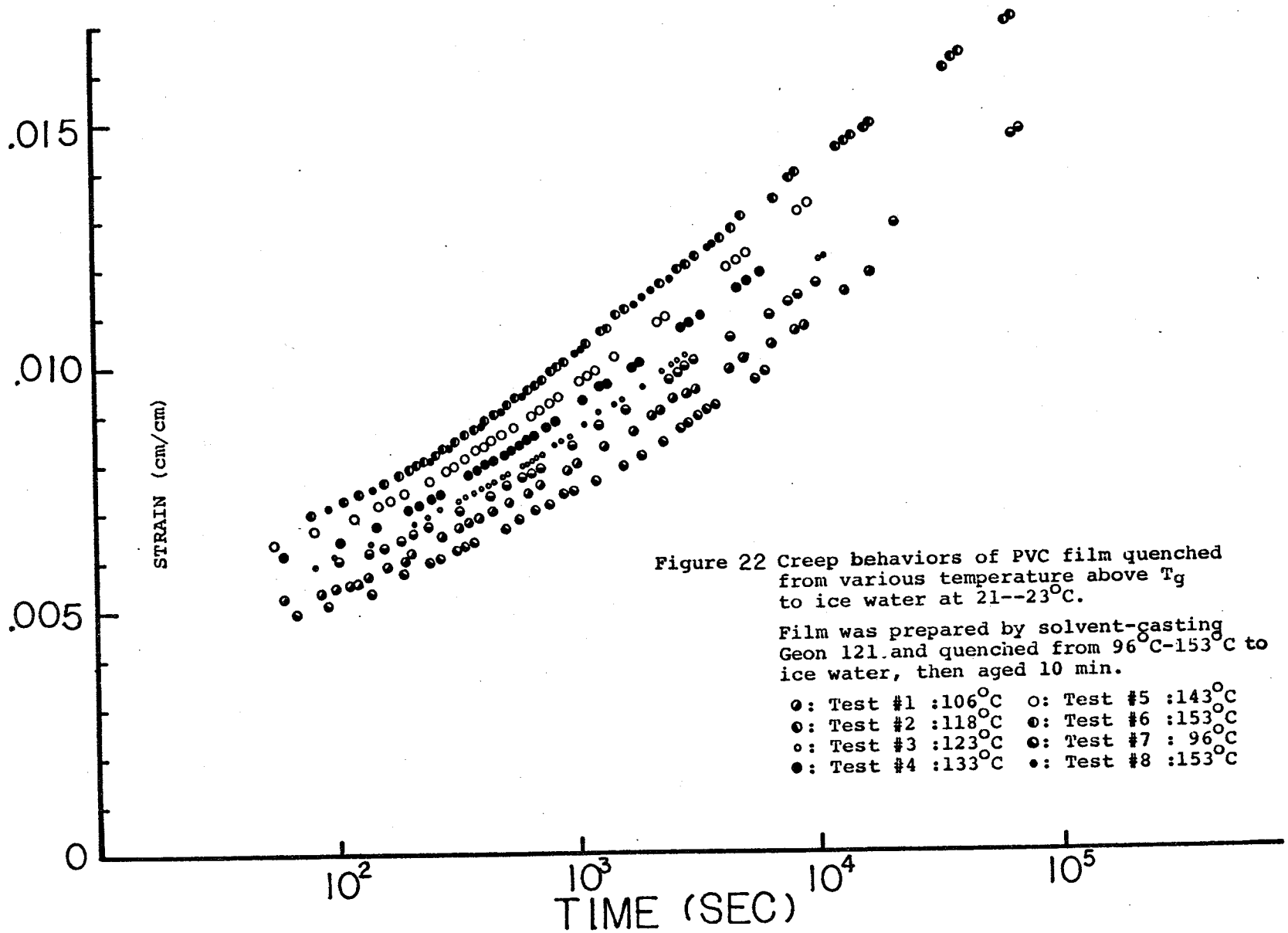

Figure 22 Creep behaviors of PVC film quenched from various temperature above T_g to ice water at 21--23°C.

Film was prepared by solvent-casting Geon 121 and quenched from 96°C-153°C to ice water, then aged 10 min.

●: Test #1 :106°C ○: Test #5 :143°C
◐: Test #2 :118°C ◐: Test #6 :153°C
○: Test #3 :123°C ◐: Test #7 : 96°C
●: Test #4 :133°C •: Test #8 :153°C

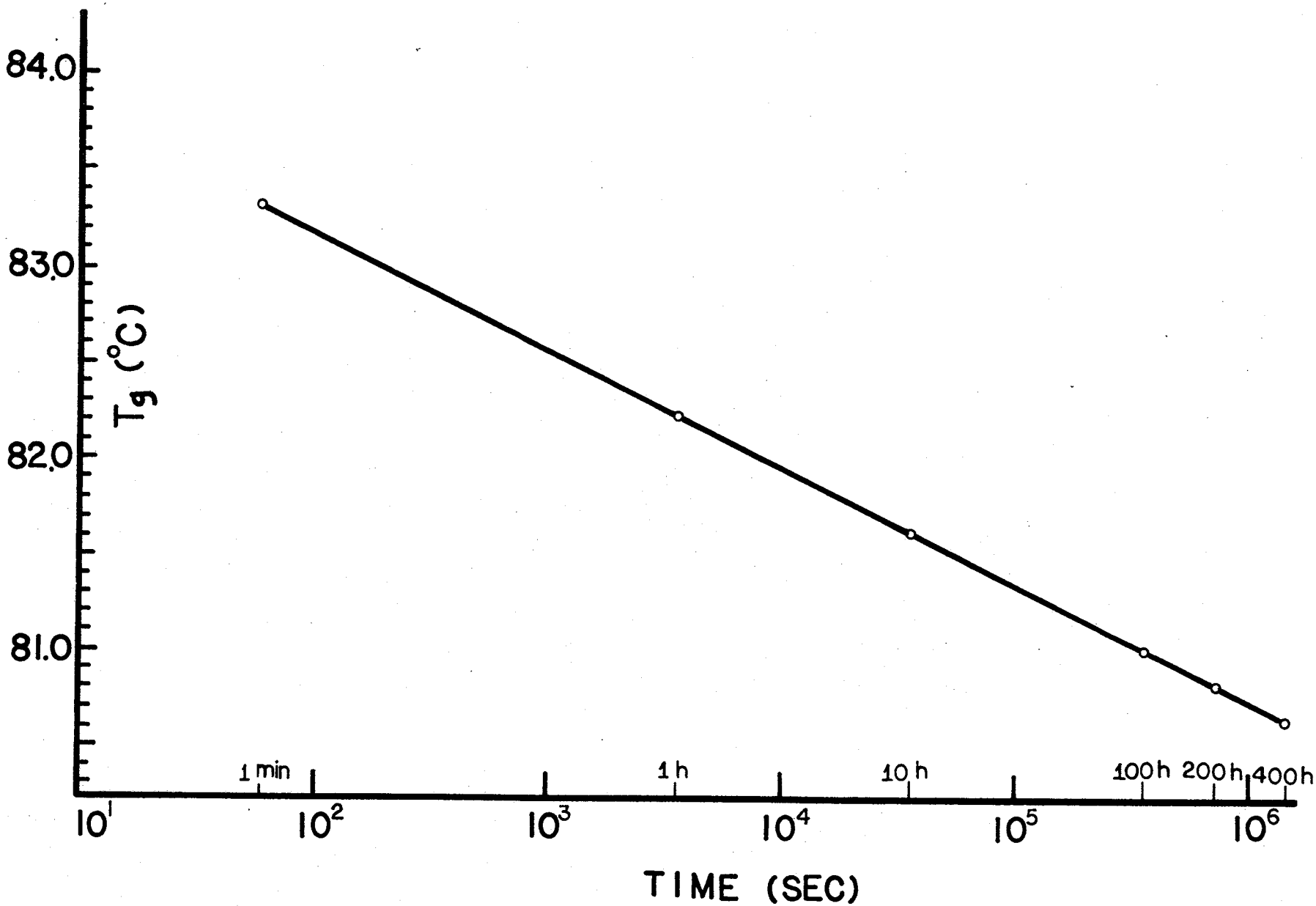
84.0
83.0
82.0
81.0
T_g (°C)
1 min
1 h
10 h
100 h
200 h
400 h
10^1
10^2
10^3
10^4
10^5
10^6
TIME (SEC)

FIG. 23

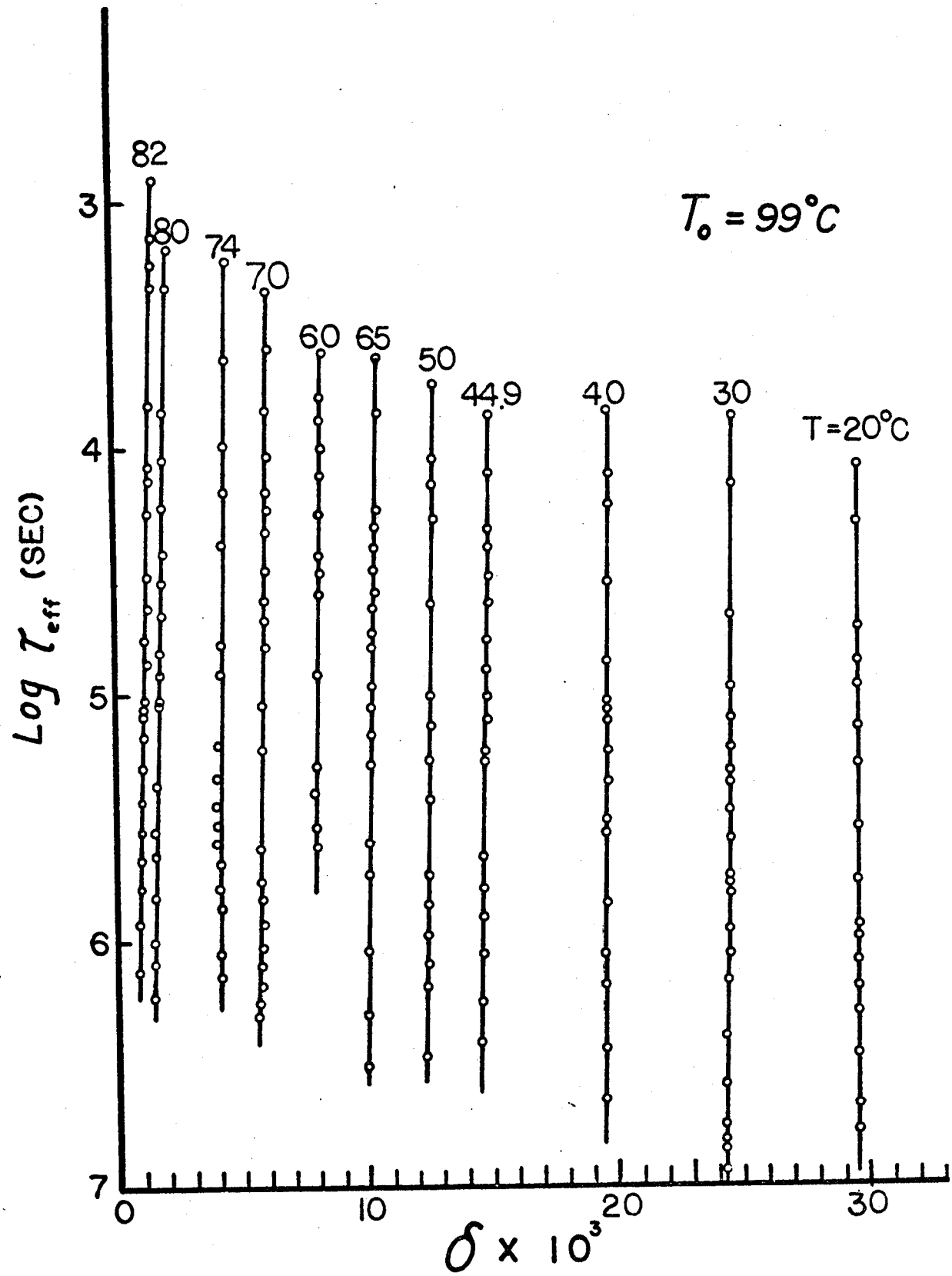
82
80
74
70
60
65
50
44.9
40
30
T=20°C
$T_0 = 99°C$
Log τ_{eff} (SEC)
3
4
5
6
7
0
10
20
30
$\delta \times 10^3$

FIG. 24

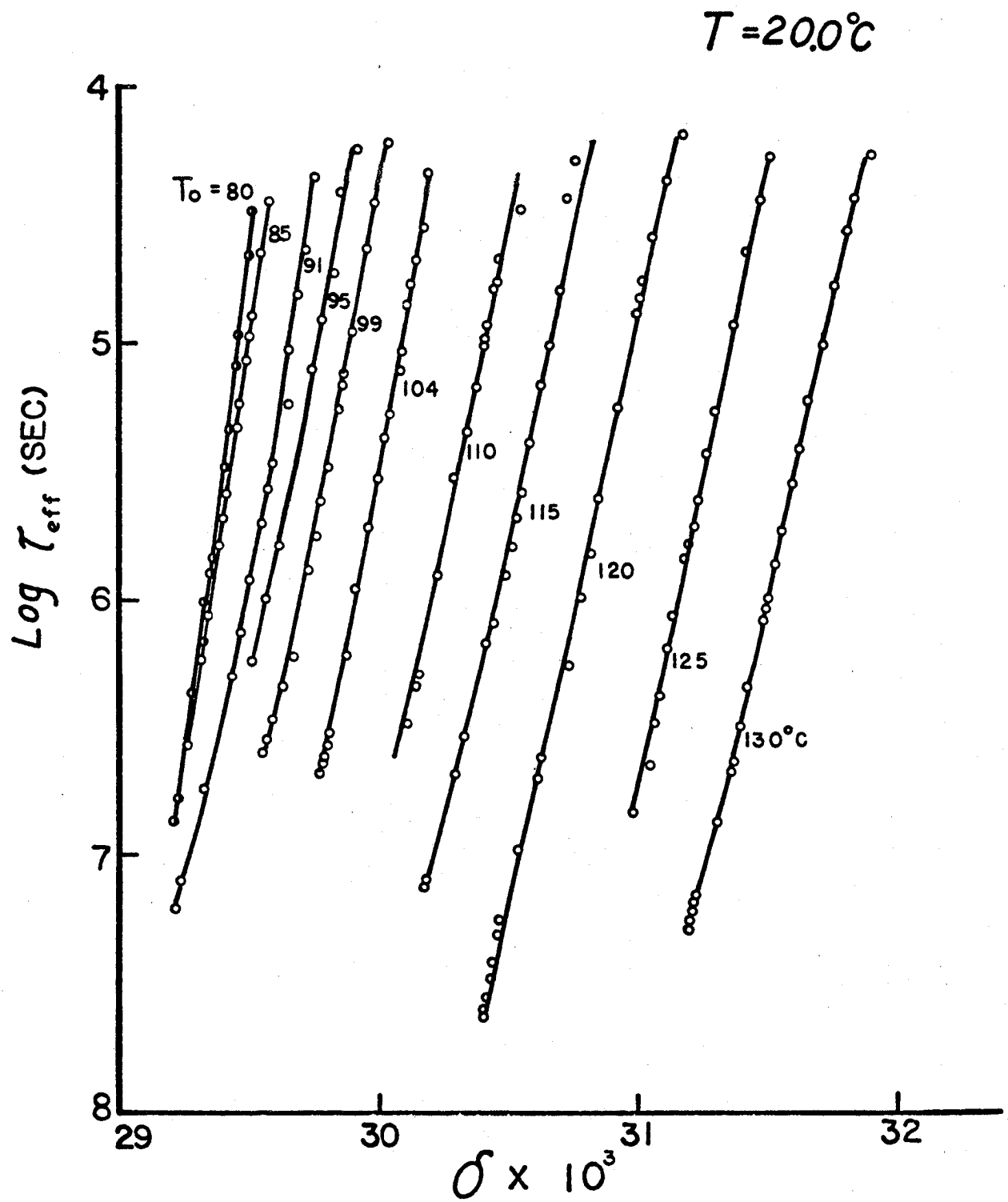
T = 20.0°C
Log τ_{eff} (SEC)
4
5
6
7
8
29
30
31
32
$\sigma \times 10^3$
T_o = 80
85
91
95
99
104
110
115
120
125
130°C

FIG. 25

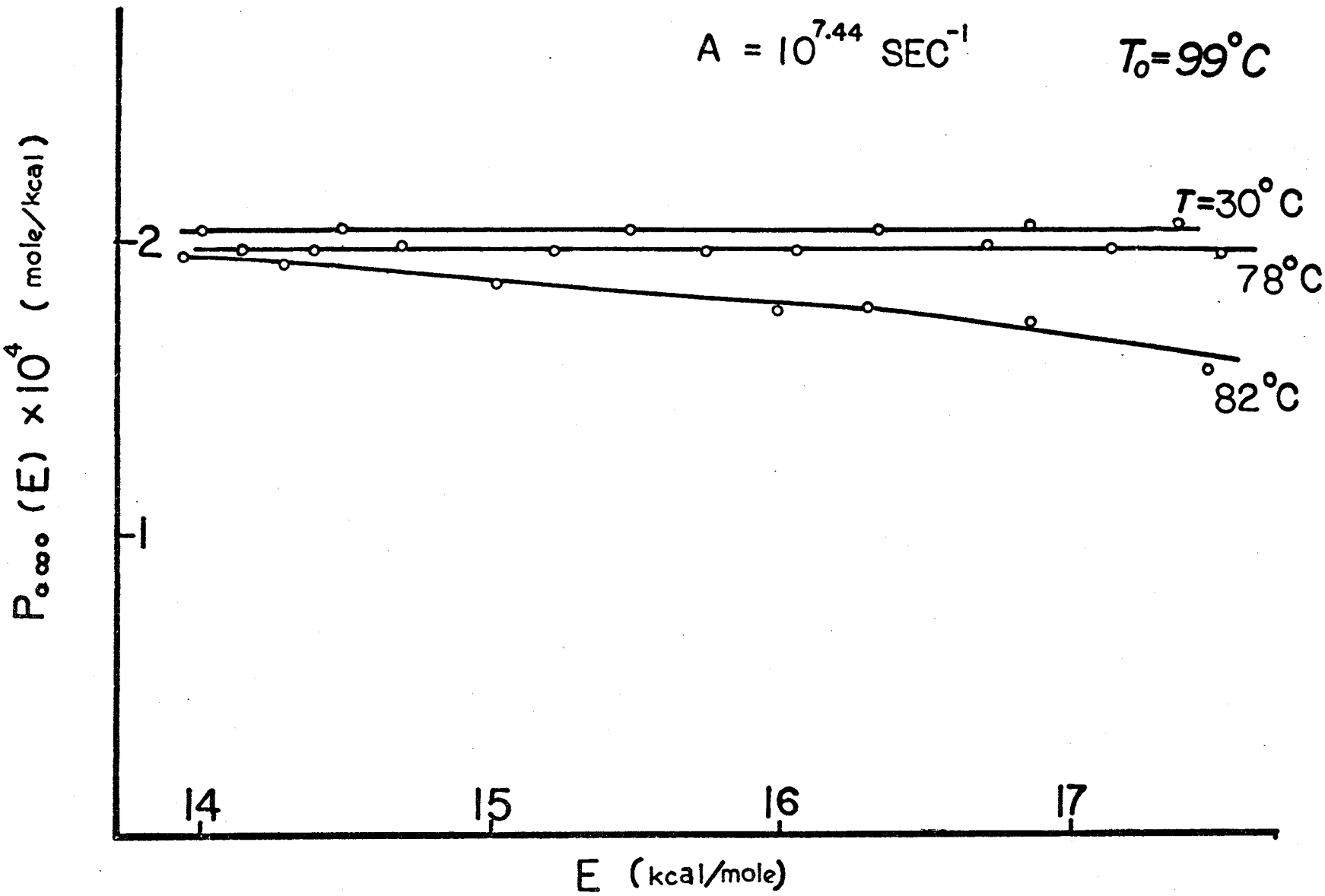
A = 10^7.44 SEC^-1
T0=99°C
T=30°C
78°C
82°C
2
1
P∞∞ (E) ×10^4 (mole/kcal)
14
15
16
17
E (kcal/mole)

FIG. 26

BIBLIOGRAPHY

1. Ananthataman, T.R.; and Suryanarayana, C.; J. of Mat. Sci., 6, 1111 (1971).

2. Jones, H., "Rapidly Quenched Metals", Grant N.J.; ed., 1, M.I.T. Press (1976).

3. Davies, H.A.; "Rapidly Quenched Metals LLL", Cantor B., ed., 2, Chameleon Press, London (1978).

4. Warlimont, H.; Phys. Technol., 11 28 (1978).

5. Gilman, J.J.; Sci. 208, 856 (1980).

6. Chaudhari, P.; Giessen, B.C.; and Turnbull, D.; Scientific American, 98 (April 1980).

7. Tool, A.Q.; J. Amer. Cer. Soc. 29, 240 (1946).

8. Tool, A.Q.; J. Res. Nat. Bur. Standards, 37, 73 (1946).

9. Schwarzl, F.R.; and Zahradnik, F.; Rheological ACTA, 19, 137 (1980).

10. Mininni, R.M.; Moore, R.S.; Flick, F.R.; and Petrie, S.E.B.; J. Macromol. Sci.-Phys., B8(1-2), 343 (1973).

11. Morgan, R.J.; and O'neal, J.E.; J. Polym. Sci., Polym. Phys. Ed., 14, 1053 (1976).

12. Hutchinson, J.M.; and Bucknall, C.B.; Polym. Eng. and Sci.; 20, 1973 (1980).

13. Kovacs, A.J.; Stratton, R.A.; and Ferry, J.D.; J. Phys. Chem.; 67, 152 (1963).

14. Struik, L.C.E.; "Physical Aging in Amorphous Polymers and Other Materials", Elsevier (1978).

15. Struik, L.C.E., Chim. Ind., 58, 549 (1976).

16. Petrie, S.E.B., Am. Chem. Soc., Div. Polym. Chem. Polym. Prepr., 15, 336 (1974).

17. Petrie, S.E.B.; Am. Macromol. Sci.-Phys., B12, 225 (1976).

18. Sherby, O.D.; and Dorn, J.E.; J. Mech. Phys. Sol., 6, 145 (1958).

19. Legrand, D.G.; J. Appl. Polym. Sci., 13, 2129 (1969).

20. Ender, D.H.; J. Macromol. Sci.-Phys., B4, 635 (1970).

21. Robertson, R.E.; and Joynson, C.W.; J. Appl. Polym. Sci., 16,733 (1972).

22. Moore, R.S.; and Petrie, S.E.B.; Am. Chem. Soc., Div. Polym. Chem. Polym. Prepr., 15, 70 (1974).

23. Williams, M.L.; Landel, R.F.; and Ferry, J.D.; J. Amer. Chem. Soc., 77, 4701 (1955).

24. Cohen, M.H.; and Turnbull, D.; J. Chem. Phys. 31, 1164 (1959).

25. Kovacs, A.J.; Rheologica ACTA, Band 5, Heft 4, 262 (1966).

26. Robertson, R.E.; J. Polym. Sci. Polym. Symp. 63, 173 (1978).

27. Robertson, R.E.; J. Polym. Sci. Polym. Phys. Ed. 17, 597 (1979).

28. Kovacs, A.J.; J. Polym. Sci., 30, 131 (1958).

29. Kovacs, A.J.; Fortschr. Hochpolym.-Forsch., Bd. 3,S.394 (1963).

30. Hutchinson, J. M.; Aklonis, J.J.; and Kovacs, A.J.; Polym. Prepr. 16(2), 94 (1975).

31. Hutchinson, J.M.; and Kovacs, A.J.; J. Polym. Sci. Polym. Phys. Ed. 14, 1575 (1976).

32. Kovacs, A.J.; Hutchinson, J.M.; and Aklonis, J.J.; Proceedings of The Symposium on the Structure of Non-crystalline Materials, Cambridge, 153 (1976).

33. Hutchinson, J.M.; and Kovacs, A.J.; Proceedings of the Symposium on The Structure of Non-crystalline Materials, Camberidge, 167 (1977).

34. Lee, H.D.; Progress Report on Rapid Quenching I, June 5, 1980.

35. Lee, H.D.; Progress Report on Rapid Quenching II, Nov. 24, 1980.

36. Bowman, H.A.; and Schoonover, R.M.; J. of Research of the National Bureau of Standard, Vo. 71C, No. 3, 179 (1967).

37. 1979, Annual Book of ASTM Standards, Part 17, C693-74.

38. 1979, Annual Book of ASTM Standards, Part 35, D792.

39. Hoffman, J.D.; and Weeks, J.J.; J of Research of The National Bureau of Standard, Vo. 60, No. 5, 465 (1958).

40. Madorsky, S.L.; Vacuum Microbalance Techniques, Vo. 2, 47 (1962).

41. Bekkedahl, N.; National Bureaf of Standards, Vo. 42, 145 (1949).

42. Onaran, K.;and Findley, W.N.; "Combined Stress Creep Experiments on A Nonlinear Viscoelastic Material to Determine The Kernel Functions for Multiple Integral Representation of Creep". Transaction of The Society of Rheology, Vol. 9, issue 2, 299,(1965).

43. Findley, W.N.; and Khosla, G.; "An Equation for Tension Creep of Three Unfilled Thermoplastics", SPE Journal, Vol. 12, 20(1956).

44. Findley, W.N.; and Peterson, D.B.; "Prediction of Long-Time Creep with Ten-year Creep Data on Four Plastic Laminates", Proceedings of ASTM, Vol. 58, 841,(1958).

45. Findley, W.N.; and Tracy, J.F.; "16-year Creep of Polyethylene and PVC", Polymer Engineering and Science, Vol. 14, 577,(1974).

46. Hutchinson, J.M.; and Kovacs, A.J.; in "The Structure of Non-Crystalline Materials", P.H. Gaskell, ED., Taylor Francis, London (1977).

47. Kovacs, A.J.; Aklonis, J.J.; Hutchinson, J.m.; and Ramos, A.R.; J. Polym. Sci. Polym. Phys. Ed., 17, 1097 (1979).

48. Vand, V.; Proc. Phys. Soc. (London) A55, 222 (1943).

49. Primak, W.; Phys. Rev. 100, 1677 (1955).

50. Primak, W.; J. Appl. Phys. 31, 1524 (1960).

51. Kimmel, R.M.; and Uhlmann, D.R.; J Appl. Phys. 40, 4254, (1969).

52. Kimmel, R.M.; and Uhlmann, D.R.; J. Appl. Phys. 41, 592 (1970).

53. Kimmel, R.M.; and Uhlmann, D.R.; J. Appl. Phys. 42 4926 (1971).

54. Straff, R.; and Uhlmann, D.R.; J. Polym. Sci., Polym. Phys. Ed., 14, 1087 (1976).

55. Steger, T.R.; Schaefer,J.; Stejskal, E.O.; Mckay, R.A.; and Sefecik, M.D.; "High Resolution Solid State NMR of Glasses".

56. Schaefer, J.; Stejskal, E.O.; and Buchadahl, R.; Macromolecules, Vo.10, 384 (1977).

57. Lyerla, Jr., J.R.; McIntyre, H.M.; and Torchia, D.A.; Macromolecules, Vo.7, 11 (1974).

58. Bunn, A.; and Cudby, M. E.A.; J.C.S. Chem. Comm., 15, (1981).